Journal of Innovative Applied Mathematics and Computational Sciences

J. Innov. Appl. Math. Comput. Sci. **5**(2) (2025), 219–252. DOI: 10.58205/jiamcs.v5i2.1956

http://jiamcs.univ-mila.dz/

Bifurcation analysis and optimal control in a predator-prey-infection model with additional food

Sudip Samanta [1] ✉, Mahammad Yasin Khan [2] and Prabir Sen [3]

[1]Department of Mathematics, Bankura University, Bankura, West Bengal 722155, India
[2]Department of Mathematics, Kabi Jagadram Roy Govt. General Degree College, Mejia, West Bengal 722143, India
[3]Department of Mathematics, Triveni Devi Bhalotia College, Raniganj, West Bengal 713347, India

Received July 12, 2025, Accepted October 8, 2025, Published January 07, 2026

Abstract. We propose and analyze a three-dimensional eco-epidemiological model involving susceptible and infected prey and predators, in which the predators are supplemented with a constant externally supplied food supply. The model incorporates nonlinear disease transmission and predator feeding saturation through a generalized Holling type II functional response. We investigate the system's dynamics analytically and numerically by examining the existence and stability of equilibria, as well as Hopf, transcritical, and saddle-node bifurcations. One- and two-parameter bifurcation analyses reveal rich dynamics, including limit cycles, period doubling, and chaotic oscillations. Our findings indicate that disease transmission can destabilize the system, while the inclusion of additional food enhances stability and can suppress chaos. Furthermore, we extend the model by introducing a time-dependent optimal control variable representing additional food supply, and derive an optimal strategy using Pontryagin's Maximum Principle. Numerical simulations show that optimal control effectively reduces disease prevalence and stabilizes population dynamics. This study highlights the potential of ecological interventions, such as strategic food supplementation, in regulating complex eco-epidemiological systems.

Keywords: Eco-epidemiology; Additional food; Optimal control; Bifurcation analysis; Chaotic oscillations; Disease eradication.

2020 Mathematics Subject Classification: 92-10, 34C23, 49-XX.

1 Introduction

Interactions among species play a pivotal role in shaping evolutionary and ecological dynamics within natural environments. In particular, predator-prey relationships have been

✉Corresponding author. Email: samanta.sudip.09@gmail.com

ISSN (electronic): 2773-4196

extensively studied across diverse ecological systems. These interactions often involve organisms and their natural adversaries, such as plant-herbivore [9], host-parasite [11], herbivore-carnivore [31], and host-pathogen [10] relationships. predator-prey dynamics directly influence the birth rate of predators and the mortality rate of prey, and govern energy flow through food chains. This relationship is central to the structure and stability of ecological communities, making it a fundamental topic in mathematical ecology.

The pioneering works of Lotka and Volterra independently introduced mathematical models of predator-prey interactions, revealing rhythmic population dynamics between predators and prey [25, 39]. Since then, modeling these dynamics has attracted significant attention from researchers [5, 12, 26, 34], leading to the development of models with various functional responses [19] that capture the primary influence of predation on ecosystem behavior.

Parasites significantly influence the structure of food webs by altering host behavior, fitness, and population abundances, thereby playing a crucial role in trophic interactions. A pioneering effort to incorporate disease dynamics into predator-prey models was made by Hadeler and Freedman [15], who introduced a framework in which prey populations could become infected by parasites. They supported their model with several biological examples. For instance, cracked skull disease has been shown to increase the susceptibility of Asian catfish species (*Clarias batrachus* and *Clarias macrocephalus*) to predation [22]. Similarly, Peterson and Page [30] reported that wolf predation on moose is more successful when the moose is heavily infected with *Echinococcus granulosus*.

In recent decades, mathematical modeling has emerged as a vital tool for analyzing and understanding the spread and control of infectious diseases, particularly when ethical or practical constraints limit experimental approaches. In such cases, modeling provides valuable insights for effective disease management and policy development. Numerous studies have incorporated disease dynamics into predator-prey frameworks to explore the effects of infection on ecological interactions [3, 4, 8, 14, 15, 17, 18, 21, 24, 27, 33, 40]. While most of these models focus on disease transmission within prey populations, a few also consider infection in predators [18, 24, 40]. A common objective across these studies is to identify strategies that often involve predation mechanisms to suppress or eliminate disease in the prey population.

It is now widely recognized that most predators engage in complex interactions with multiple prey species, rather than relying on a single prey type [38]. Many of these predators exhibit migratory behavior, often operating across geographical scales much larger than those of individual prey populations. As a result, the presence of alternative prey must be considered to develop realistic and ecologically accurate predator-prey models.

Holt and Lawton [20] emphasized that the impact of generalist predators is influenced not only by the abundance and vulnerability of primary prey, but also by the presence and density of alternative prey. Consequently, understanding the relative contributions of direct and indirect effects in multi-species predator-prey systems is essential for accurately predicting the dynamics of complex food webs.

The ecological roles of predators and their influence on prey-predator dynamics have long intrigued scientists, particularly regarding their contributions to biological regulation [7, 28, 42]. Motivated by this, the present study introduces an additional prey species-assumed to be available at a constant density-into a previously studied predator-prey model, thereby expanding the system's complexity.

While the dynamics of classical models involving a single predator and a single prey are well understood, extensions that include alternative food sources provide a more realistic framework. Abrams and Roth [1] discussed several theoretical models involving higher

trophic levels. Our model incorporates an alternative prey species, aiming to capture the dynamics of an extended predator-prey system. This approach results in a system that is more manageable than full three-species models, yet rich enough to exhibit complex behaviors [6, 13].

Notable related works include Roy et al. [32], who analyzed an exploitative system involving two prey species and one predator. Spencer and Collie [35] examined a prey-predator fish model with alternative prey in the context of harvesting, observing that when the abundance of primary prey was low, predator numbers could still increase due to the availability of alternative prey.

Similarly, Srinivasu et al. [36] developed a two-dimensional predator-prey model incorporating additional food sources, examining the effects of food quality on system dynamics. Building upon this, Srinivasu and Prasad [37] applied bang-bang control theory to drive the system toward a desired equilibrium efficiently via controlled food supplementation. Kar and Chattopadhyay [23] also explored a harvested predator-prey system with multiple prey types, further emphasizing the ecological and mathematical relevance of alternative food sources. Recently, Akhter et al. [2] have explored complex dynamics of a tri-trophic food chain model with toxicity and additional food.

In this study, we investigate a predator-prey model in which the prey population is subject to an infectious disease, and the predator consumes both susceptible and infected prey. In addition, the predator has access to an alternative food source, assumed to be available at a constant density. The predator's feeding behavior is modeled using a generalized Holling type II functional response, where all three food sources-susceptible prey, infected prey, and alternative food-contribute to feeding saturation. The primary aim of this work is to analyze the influence of disease transmission on population dynamics and community structure, and to explore how the inclusion of additional food affects the system's stability, persistence, and potential to suppress chaotic behavior.

In the latter part of this study, we extend the model by incorporating a time-dependent optimal control variable representing the supply of additional food to predators. This control framework aims to minimize the infection burden in the prey population while balancing the cost of intervention and the sustainability of the predator population. Using Pontryagin's Maximum Principle, we derive necessary optimality conditions and analyze the corresponding state and adjoint systems. Numerical simulations confirm that the optimal control strategy not only suppresses infection effectively but also stabilizes the overall population dynamics. This highlights the potential of ecological resource management as a viable tool for disease mitigation in complex predator-prey-infection systems.

2 Model formulation

The primary objective of this study is to investigate the dynamic behavior of a biological system involving disease transmission in a prey population, where predators feed on both susceptible and infected prey. Additionally, the predators are supplemented with an external constant food source.

We construct a predator-prey model in which the prey population is divided into two subgroups: susceptible prey (S) and infected prey (I). The predator population is denoted by P. We assume that the susceptible prey grow logistically, whereas the infected prey do not reproduce. Disease transmission among prey follows a Holling type II functional response and occurs at a rate β. Predators are assumed to be immune to the infection.

Predators consume both susceptible and infected prey, but at different rates, denoted by α_1 and α_2, respectively. Following the strategy of Srinivasu *et al.* [36], we assume that the predator's total intake also includes an externally supplied, constant quantity of additional food A. We consider a scenario of steady provisioning, akin to a management practice in which rangers or farmers supply a fixed amount of food daily, ensuring that predators always have access to the same level of supplementary food. Introducing a dynamic additional food supply would require formulating an additional differential equation for the food itself, thereby increasing the system's dimensionality and mathematical complexity. To avoid such complications, we assume that further food is supplied at a constant rate. The combined intake from all food sources-susceptible prey, infected prey, and extra food is assumed to saturate the predator's consumption rate according to a generalized Holling type II functional response.

For analytical simplicity, we assume the additional food supply A remains constant over time and exclude it from dynamic modeling. This allows us to focus on how a fixed external resource influences the overall system dynamics.

The model is governed by the following system of ordinary differential equations:

$$\begin{aligned}
\frac{dS}{dt} &= aS - bS^2 - cSI - \frac{\beta SI}{\delta + S} - \frac{\alpha_1 SP}{1 + \gamma_1 S + \gamma_2 I + \lambda\eta A}, \\
\frac{dI}{dt} &= \frac{\beta SI}{\delta + S} - \frac{\alpha_2 IP}{1 + \gamma_1 S + \gamma_2 I + \lambda\eta A} - \mu I, \\
\frac{dP}{dt} &= \frac{(e_1\alpha_1 S + e_2\alpha_2 I + e_3\eta A)P}{1 + \gamma_1 S + \gamma_2 I + \lambda\eta A} - mP.
\end{aligned} \tag{2.1}$$

System (2.1) shall be investigated with the initial values: $S(0) > 0, I(0) > 0, P(0) > 0$. The parameters and their interpretations are given in the Table 2.1.

Table 2.1: Description of parameters used in model (2.1).

Parameters	Description
a	intrinsic growth rate of the susceptible prey
b	intra-specific competition rate among susceptible prey
c	interspecific competition between susceptible and infected prey
β	disease transmission rate among prey
δ	half-saturation constant for disease transmission
α_1, α_2	predation rates on susceptible and infected prey
γ_1, γ_2	parameters representing prey interference or handling times
λ, η	scaling factors for the effect of additional food
A	constant density of additional food provided externally

3 Preliminary results

3.1 Boundedness

Due to resource limitations in nature, no species can grow indefinitely. Therefore, it is important to demonstrate that the solutions of our model are bounded, ensuring biological feasibil-

ity.

Lemma 3.1. *All the solutions of the system (2.1) initiate in R^3_+ are uniformly bounded.*

Proof. Let q be an arbitrary positive constant such that $0 < q \leq \min\{\mu, m\}$. Define the total population function $W = S + I + P$. Taking the derivative with respect to time and using the system equations, we obtain:

$$\begin{aligned}
\frac{dW}{dt} &= \frac{dS}{dt} + \frac{dI}{dt} + \frac{dP}{dt} \\
&= aS - bS^2 - cSI + (e_1 - 1)\frac{\alpha_1 SP}{1 + \gamma_1 S + \gamma_2 I + \delta\eta A} + (e_2 - 1)\frac{\alpha_2 IP}{1 + \gamma_1 S + \gamma_2 I + \delta\eta A} \\
&\quad + \frac{e_3 \eta A}{1 + \gamma_1 S + \gamma_2 I + \delta\eta A} - \mu I - mP \\
\Rightarrow \frac{dW}{dt} &\leq (aS - bS^2 - cSI - \mu I - mP), \\
&\text{where } 0 < e_1, e_2, e_3 \leq 1. \\
\Rightarrow \frac{dW}{dt} + qW &\leq aS\left(1 - \frac{bS}{a} + \frac{q}{a}\right) + qW + \eta A \\
\Rightarrow \frac{dW}{dt} + qW &\leq aS\left(1 - \frac{bS}{a} + \frac{q}{a}\right) + \eta A - (\mu - q)I - (m - q)P \\
\Rightarrow \frac{dW}{dt} + qW &\leq aS\left(1 - \frac{bS}{a} + \frac{q}{a}\right) + \eta A, \text{ since we have considered } 0 < q \leq min\{\mu, m\}. \\
&\leq b\left[\frac{a}{b}\left(1 + \frac{q}{a}\right)S - S^2\right] + \eta A \\
&\leq b\left[\left(\frac{a+q}{2b}\right)^2 - \left(S - \frac{a+q}{2b}\right)^2\right] + \eta A \\
&\leq \frac{(a+q)^2}{4b} + \eta A.
\end{aligned}$$

Applying the theory of differential inequality [16], we obtain

$$0 < W(S, I, P) \leq \frac{(a+q)^2}{4b} + \eta A + e^{-qt}\left[W(S(0), I(0), P(0)) - \left(\frac{(a+q)^2}{4b} + \eta A\right)\right].$$

For $t \to \infty$, $0 < W \leq \frac{(a+q)^2}{4b} + \eta A$. Hence, the system is bounded. □

3.2 Permanence

From a biological standpoint, permanence ensures the long-term survival of all species regardless of initial population sizes. Mathematically, it implies that all population variables remain strictly positive over time and do not approach zero asymptotically.

Dissipativeness: From Lemma 3.1, we observe that the linear sum of the state variables (i.e. $S + I + P$) is bounded above. Without loss of generality we can assume that $S + I + P \leq M$, where $M > 0$ is a real constant. Therefore, each component (state variable) of the system is bounded above i.e. $S,\ I,\ P \leq M$. Hence, the system (2.1) is dissipative.

Permanence: From the system (2.1), we can easily obtain the following Kolmogorov type

inequation

$$\begin{aligned}\frac{dS}{dt} &\geq S\left(a - bS - cI - \frac{\beta}{\delta}I - \alpha_1 P\right),\\ \frac{dI}{dt} &\geq I\left(\frac{\beta S}{\delta + M} - \alpha_2 P - \mu\right),\\ \frac{dP}{dt} &\geq P\left(\frac{e_1\alpha_1 S}{(1+\gamma_1 M + \gamma_2 M + \lambda\eta A)} - m\right).\end{aligned} \tag{3.1}$$

Let (w_1, w_2, w_3) be the positive root of the system of the equation

$$\begin{aligned}a - bS - cI - \frac{\beta}{\delta}I - \alpha_1 P &= 0\\ \frac{\beta S}{\delta + M} - \alpha_2 P - \mu &= 0\\ \frac{e_1\alpha_1 S}{(1+\gamma_1 M + \gamma_2 M + \lambda\eta A)} - m &= 0.\end{aligned} \tag{3.2}$$

Using the standard comparison theorem [16], we observe that the above inequality (3.1) implies

$$\liminf_{t\to\infty} S(t) \geq w_1,\ \liminf_{t\to\infty} I(t) \geq w_2,\ \liminf_{t\to\infty} P(t) \geq w_3$$

with

$$w_1 = \frac{m(1 + A\eta\lambda + \gamma_1 M + \gamma_2 M)}{\alpha_1 e_1},$$

$$w_2 = \frac{\delta(a\alpha_2 + \alpha_1\mu)}{\alpha_2(\beta + c\delta)} - \frac{\delta m(\alpha_1\beta + \alpha_2 b\delta + \alpha_2 bM)(1 + A\eta\lambda + \gamma_1 M + \gamma_2 M)}{\alpha_1\alpha_2 e_1(\beta + c\delta)(\delta + M)},$$

$$w_3 = \frac{\beta m(1 + A\eta\lambda + \gamma_1 M + \gamma_2 M)}{\alpha_1\alpha_2 e_1(\delta + M)} - \frac{\mu}{\alpha_2}.$$

Lemma 3.2. *The system (2.1) is permanent i.e.,* $\liminf_{t\to\infty} S(t) \geq w_1$, $\liminf_{t\to\infty} I(t) \geq w_2$, $\liminf_{t\to\infty} P(t) \geq w_3$ *if* $\delta(a\alpha_2 + \alpha_1\mu) > \frac{\delta m(\alpha_1\beta + \alpha_2 b\delta + \alpha_2 bM)(1 + A\eta\lambda + \gamma_1 M + \gamma_2 M)}{\alpha_1 e_1(\delta + M)}$ *and* $\frac{\beta m(1 + A\eta\lambda + \gamma_1 M + \gamma_2 M)}{\alpha_1 e_1(\delta + M)} > \mu$.

4 Stability and bifurcation analysis

4.1 Existence of the equilibria

System (2.1) has at most five equilibrium points, they are following
(i) The trivial equilibrium point $E_0(0, 0, 0)$ always exists.
(ii) The axial equilibrium point $E_1(\frac{a}{b}, 0, 0)$ is also existing always since $b > 0$ according to our hypothesis.
(iii) The disease-free equilibrium $E_2(S_2, 0, P_2)$ where $S_2 = \frac{m(1 + \lambda\eta A) - e_3\eta A}{(e_1\alpha_1 - m\gamma_1)}$ and $P_2 = \frac{(ae_1\alpha_1 - am\gamma_1 - bm - bm\lambda\eta A + e_3 b\eta A)(e_1\alpha_1 - e_3\gamma_1\eta A + e_1\alpha_1\lambda\eta A)}{\alpha_1(e_1\alpha_1 - m\gamma_1)^2}$ providing the given condition.
(iv) The predator-free equilibrium $E_3(S_3, I_3, 0)$ where $S_3 = \frac{\mu\delta}{\beta - \mu}$ and $I_3 = \frac{\delta(a\beta - a\mu - b\mu\delta)}{(c\delta + \beta - \mu)(\beta - \mu)}$, provided the given condition $\beta > \mu$ and $a\beta > \mu(a + b\delta)$.

(v) The interior equilibrium point is given by $E^*(S^*, I^*, P^*)$, where S^*, I^*, P^* are positive and satisfy the following relations

$$\begin{aligned} a - bS - cI - \frac{\beta I}{\delta + S} - \frac{\alpha_1 P}{1 + \gamma_1 S + \gamma_2 I + \lambda\eta A} &= 0, \\ \frac{\beta S}{\delta + S} - \frac{\alpha_2 P}{1 + \gamma_1 S + \gamma_2 I + \lambda\eta A} - \mu &= 0, \\ \frac{e_1\alpha_1 S + e_2\alpha_2 I + e_3\eta A}{1 + \gamma_1 S + \gamma_2 I + \lambda\eta A} - m &= 0. \end{aligned} \tag{4.1}$$

4.2 Local stability analysis

The Jacobian matrix for the system (2.1) at any arbitrary equilibrium point $E(S, I, P)$ is

$$J = \begin{pmatrix} m_{11} & m_{12} & m_{13} \\ m_{21} & m_{22} & m_{23} \\ m_{31} & m_{32} & m_{33} \end{pmatrix},$$

where

$$\begin{aligned} m_{11} &= a - 2bS - cI + \frac{\beta SI}{(\delta + S)^2} - \frac{\beta I}{\delta + S} + \frac{\alpha_1\gamma_1 SP}{(1 + \gamma_1 S + \gamma_2 I + \lambda\eta A)^2} - \frac{\alpha_1 P}{1 + \gamma_1 S + \gamma_2 I + \lambda\eta A}, \\ m_{12} &= -cS - \frac{\beta S}{\delta + S} + \frac{\alpha_1\gamma_2 SP}{(1 + \gamma_1 S + \gamma_2 I + \lambda\eta A)^2}, \; m_{13} = -\frac{\alpha_1 S}{1 + \gamma_1 S + \gamma_2 I + \lambda\eta A}, \\ m_{21} &= \frac{\beta I}{\delta + S} - \frac{\beta SI}{(\delta + S)^2} + \frac{\alpha_2\gamma_1 IP}{(1 + \gamma_1 S + \gamma_2 I + \lambda\eta A)^2}, \\ m_{22} &= \frac{\beta S}{\delta + S} - \frac{\alpha_2 P}{1 + \gamma_1 S + \gamma_2 I + \lambda\eta A} + \frac{\alpha_2\gamma_2 IP}{(1 + \gamma_1 S + \gamma_2 I + \lambda\eta A)^2} - \mu, \\ m_{23} &= -\frac{\alpha_2 I}{1 + \gamma_1 S + \gamma_2 I + \lambda\eta A}, \; m_{31} = \frac{e_1\alpha_1 P}{1 + \gamma_1 S + \gamma_2 I + \lambda\eta A} - \frac{(e_1\alpha_1 S + e_2\alpha_2 I + e_3\eta A)\gamma_1 P}{(1 + \gamma_1 S + \gamma_2 I + \lambda\eta A)^2}, \\ m_{32} &= \frac{e_2\alpha_2 P}{1 + \gamma_1 S + \gamma_2 I + \lambda\eta A} - \frac{(e_1\alpha_1 S + e_2\alpha_2 I + e_3\eta A)\gamma_2 P}{(1 + \gamma_1 S + \gamma_2 I + \lambda\eta A)^2}, \; m_{33} = \frac{e_1\alpha_1 S + e_2\alpha_2 I + e_3\eta A}{1 + \gamma_1 S + \gamma_2 I + \lambda\eta A} - m. \end{aligned}$$

Lemma 4.1. *The equilibrium point E_0 is always a saddle.*

Proof. The eigenvalues of the Jacobian matrix for E_0 are a, $-\mu$, and $-m$. Hence, E_0 is always a saddle since $a > 0$. □

Lemma 4.2. *The equilibrium point $E_1\left(\frac{a}{b}, 0, 0\right)$ is always a saddle.*

Proof. The eigenvalues of the Jacobian matrix for equilibrium point $E_1\left(\frac{a}{b}, 0, 0\right)$ are $-a$, $\frac{a\beta}{a + b\delta}$ and $\frac{e_1\alpha_1 a + \eta bA}{b + a\gamma_1 + \lambda\eta bA} - m$. Since a is always positive according to hypothesis of our model, one eigenvalue is always negative $(-a)$, while another eigenvalue is always positive $\left(\frac{a\beta}{a + b\delta}\right)$. Therefore, E_1 is a saddle. □

Lemma 4.3. *The disease-free equilibrium point $E_2(S_2, 0, P_2)$ is locally asymptotically stable if $\Delta_1 > 0, \Delta_2 > 0$ and $\Delta_1\Delta_2 > \Delta_3$, where the expression of Δ_i's are given below.*

Proof. The Jacobian matrix associated with equilibrium point $E_2(S_2, 0, P_2)$ is

$$J(E_2) = \begin{pmatrix} a_{11} & a_{12} & a_{13} \\ a_{21} & a_{22} & a_{23} \\ a_{31} & a_{32} & a_{33} \end{pmatrix},$$

where

$a_{11} = a - 2bS_2 - \dfrac{\alpha_1 S_2 P_2 \gamma_1}{(1+\gamma_1 S_2 + \lambda\eta A)^2} + \dfrac{\alpha_1 P_2}{1+\gamma_1 S_2 + \lambda\eta A}$, $a_{12} = -cs_2 - \dfrac{\beta S_2}{\delta + S_2} + \dfrac{\alpha_1 S_2 P_2 \gamma_2}{(1+\gamma_1 S_2 + \lambda\eta A)^2}$,
$a_{13} = -\dfrac{\alpha_1 S_2}{1+\gamma_1 S_2 + \lambda\eta A}$, $a_{21} = 0$, $a_{22} = \dfrac{\beta S_2}{\delta + S_2} - \dfrac{\alpha_2 P_2}{1+\gamma_1 S_2 + \lambda\eta A - \mu}$, $a_{23} = 0$,
$a_{31} = \dfrac{e_1\alpha_1 P_2}{1+\gamma_1 S_2 + \lambda\eta A} - \dfrac{(e_1\alpha_1 S_2 + \eta A)P_2\gamma_1}{(1+\gamma_1 S_2 + \lambda\eta A)^2}$, $a_{32} = \dfrac{e_2\alpha_2 P_2}{1+\gamma_1 S_2 + \lambda\eta A} - \dfrac{(e_1\alpha_1 S_2 + \eta A)P_2\gamma_2}{(1+\gamma_1 S_2 + \lambda\eta A)^2}$,
$a_{33} = \dfrac{e_1\alpha_1 S_2 + \eta A}{1+\gamma_1 S_2 + \lambda\eta A} - m.$

The characteristic equation of the Jacobian matrix $J(E_2)$ around the disease-free equilibrium point $E_2(S_2, 0, P_2)$ is

$$\chi^3 + \Delta_1\chi^2 + \Delta_2\chi + \Delta_3 = 0,$$

where the coefficients are

$$\Delta_1 = -a_{11} + a_{22} + a_{33},\ \Delta_2 = a_{11}a_{22} + a_{22}a_{33} + a_{11}a_{33},\ \Delta_3 = a_{13}a_{21}a_{22} - a_{11}a_{22}a_{33}.$$

The equilibrium point $E_2(S_2, 0, P_2)$ will be locally asymptotically stable if the coefficients of the characteristic equation satisfy the Routh-Hurwitz stability criterion *i.e.*, if $\Delta_1 > 0, \Delta_2 > 0$ and $\Delta_1\Delta_2 > \Delta_3$. □

Lemma 4.4. *The predator-free equilibrium point $E_3(S_3, I_3, 0)$ is locally asymptotically stable if $A_1 > 0, A_2 > 0$ and $A_1A_2 > A_3$, where the expression of A_i's are given below.*

Proof. The Jacobian matrix associated with equilibrium point $E_3(S_3, I_3, 0)$ is

$$J(E_3) = \begin{pmatrix} b_{11} & b_{12} & b_{13} \\ b_{21} & b_{22} & b_{23} \\ b_{31} & b_{32} & b_{33} \end{pmatrix},$$

where

$b_{11} = a - 2bS_3 - cI_3 + \dfrac{\beta S_3 I_3}{(\delta + S_3)^2} - \dfrac{\beta I_3}{\delta + S_3}$, $b_{12} = -cs_3 - \dfrac{\beta S_3}{\delta + S_3}$, $b_{13} = -\dfrac{\alpha_1 S_3}{1+\gamma_1 S_3 + \gamma_2 I_3 + \lambda\eta A}$,
$b_{21} = \dfrac{\beta I_3}{\delta + S_3} - \dfrac{\beta S_3 I_3}{(\delta + S_3)^2}$, $b_{22} = \dfrac{\beta S_3}{\delta + S_3}$, $b_{23} = -\dfrac{\alpha_2 I_3}{1+\gamma_1 S_3 + \gamma_2 I_3 + \lambda\eta A}$, $b_{31} = 0$, $b_{32} = 0$,
$b_{33} = \dfrac{e_1\alpha_1 S_3 + e_2\alpha_2 I_3 + \eta A}{1+\gamma_1 S_3 + \gamma_2 I_3 + \lambda\eta A} - m.$

The characteristic equation of the Jacobian matrix $J(E_3)$ around the predator-free equilibrium point $E_3(S_3, I_3, 0)$ is
$\xi^3 + A_1\xi^2 + A_2\xi + A_3 = 0$,
where the coefficients are
$A_1 = -b_{11} - b_{22} - b_{33}$, $A_2 = b_{11}b_{22} + b_{22}b_{33} + b_{11}b_{33}$, $A_3 = b_{12}b_{21}b_{33} - b_{11}b_{12}b_{33}$.

The equilibrium point $E_3(S_3, I_3, 0)$ will be locally asymptotically stable if the coefficients of the characteristic equation satisfy the Routh-Hurwitz stability criterion *i.e.*, if $A_1 > 0, A_2 > 0$ and $A_1A_2 > A_3$. □

Lemma 4.5. *The interior equilibrium $E^*(S^*, I^*, P^*)$ is locally asymptotically stable if $\psi_1 > 0, \psi_2 > 0$ and $\psi_1\psi_2 > \psi_3$, where the expression of ψ_i's are given below.*

Proof. The Jacobian for interior equilibrium $E^*(S^*, I^*, P^*)$ is

$$J(E^*) = \begin{pmatrix} c_{11} & c_{12} & c_{13} \\ c_{21} & c_{22} & c_{23} \\ c_{31} & c_{32} & c_{33} \end{pmatrix},$$

where,

$$c_{11} = a - 2bS^* - cI - \frac{\beta I^*}{\delta + S^*} + \frac{\beta S^* I^*}{(\delta + S^*)^2} - \frac{\alpha_1 P^*}{1 + \gamma_1 S^* + \gamma_2 I^* + \lambda\eta A} + \frac{\alpha_1\gamma_1 S^* P^*}{(1 + \gamma_1 S^* + \gamma_2 I^* + \lambda\eta A)^2},$$
$$c_{12} = -cS^* - \frac{\beta S^*}{\delta + S^*} + \frac{\alpha_1\gamma_2 S^* P^*}{(1 + \gamma_1 S^* + \gamma_2 I^* + \lambda\eta A)^2}, c_{13} = -\frac{\alpha_1 S^*}{1 + \gamma_1 S^* + \gamma_2 I^* + \lambda\eta A},$$
$$c_{21} = \frac{\beta I^*}{\delta + S^*} - \frac{\beta S^* I^*}{(\delta + S^*)^2} + \frac{\alpha_2\gamma_1 I^* P^*}{(1 + \gamma_1 S^* + \gamma_2 I^* + \lambda\eta A)^2},$$
$$c_{22} = \frac{\beta S^*}{\delta + S^*} - \frac{\alpha_2 P^*}{1 + \gamma_1 S^* + \gamma_2 I^* + \lambda\eta A} + \frac{\alpha_2\gamma_2 I^* P^*}{(1 + \gamma_1 S^* + \gamma_2 I^* + \lambda\eta A)^2} - \mu, c_{23} = -\frac{\alpha_2 I^*}{1 + \gamma_1 S^* + \gamma_2 I^* + \lambda\eta A},$$
$$c_{31} = \frac{e_1\alpha_1 P^*}{1 + \gamma_1 S^* + \gamma_2 I^* + \lambda\eta A} - \frac{(e_1\alpha_1 S^* + e_2\alpha_2 I^* + e_3\eta A)\gamma_1 P^*}{(1 + \gamma_1 S^* + \gamma_2 I^* + \lambda\eta A)^2},$$
$$c_{32} = \frac{e_2\alpha_2 P^*}{1 + \gamma_1 S^* + \gamma_2 I^* + \lambda\eta A} - \frac{(e_1\alpha_1 S^* + e_2\alpha_2 I^* + e_3\eta A)\gamma_2 P^*}{(1 + \gamma_1 S^* + \gamma_2 I^* + \lambda\eta A)^2}, c_{33} = \frac{e_1\alpha_1 S^* + e_2\alpha_2 I^* + e_3\eta A}{1 + \gamma_1 S^* + \gamma_2 I^* + \lambda\eta A} - m.$$

The characteristic equation of the Jacobian matrix $J(E^*)$ around the interior equilibrium point $E^*(S^*, I^*, P^*)$ is

$$\chi^3 + \psi_1\chi^2 + \psi_2\chi + \psi_3 = 0, \tag{4.2}$$

where the coefficients are
$\psi_1 = -c_{11} - c_{22} - c_{33}$, $\psi_2 = c_{11}a_{22} + c_{22}c_{33} + c_{11}c_{33} - c_{12}c_{21} - c_{13}c_{31} - c_{23}c_{32}$,
$\psi_3 = c_{11}c_{23}c_{32} + c_{12}c_{21}c_{33} + c_{13}c_{22}c_{31} - c_{11}c_{22}c_{33} - c_{12}c_{31}c_{23} - c_{13}c_{21}c_{32}$.

The interior equilibrium point $E^*(S^*, I^*, P^*)$ will be locally asymptotically stable if the coefficients of the characteristic equation satisfies the Routh-Hurwitz stability criterion *i.e.* if $\psi_1 > 0, \psi_2 > 0$ and $\psi_1\psi_2 > \psi_3$. □

4.3 Hopf bifurcation analysis

Theorem 4.6. *The system (2.1) undergoes a Hopf bifurcation around the interior equilibrium when the rate of disease transmission (β) exceeds a critical value. The Hopf bifurcation occurs at $\beta = \beta_H$ if*

and only if the following conditions hold

(i) $G(\beta_H) \equiv \psi_1(\beta_H)\psi_2(\beta_H) - \psi_3(\beta_H) = 0$
(ii) $\frac{d}{d\beta}(Re(\chi(\beta))|_{\beta=\beta_H} \neq 0$

where χ *is the root of the characteristic equation defined in equation (4.2).*

Proof. Let $\beta = \beta_H$, then the characteristic equation $\chi^3 + \psi_1\chi^2 + \psi_2\chi + \psi_3 = 0$ turns into $(\chi^2 + \psi_2)(\chi + \psi_1) = 0$.
Clearly, the roots of the above equation are $\chi_1 = i\sqrt{\psi_2}$, $\chi_2 = -i\sqrt{\psi_2}$ and $\chi_3 = -\psi_1$.

Now we can rewrite the roots considering λ as a bifurcation parameter as follows

$\chi_1(\beta) = \theta_1(\beta) + i\theta_2(\beta)$,
$\chi_2(\beta) = \theta_1(\beta) - i\theta_2(\beta)$,
$\chi_3(\beta) = -\psi_1(\beta)$.

Substituting $\chi_1(\beta) = \theta_1(\beta) + i\theta_2(\beta)$ into the above characteristic equation and then differentiating with respect to β and separating the real and imaginary parts, we get

$P(\beta)\theta_1'(\beta) - Q(\beta)\theta_2'(\beta) + U(\beta) = 0$,
$Q(\beta)\theta_1'(\beta) + P(\beta)\theta_2'(\beta) + V(\beta) = 0$,

where,

$P(\beta) = 3\theta_1^2(\beta) + 2\psi_1(\beta)\theta_1(\beta) + \psi_2(\beta) - 3\theta_2^2(\beta)$,
$Q(\beta) = 6\theta_1(\beta)\theta_2(\beta) + 2\psi_1(\beta)\theta_2(\beta)$,
$U(\beta) = \theta_1^2(\beta)\psi_1'(\beta) + \psi_2'(\beta)\theta_1(\beta) + \psi_3'(\beta) - \psi_1'(\beta)\theta_2^2(\beta)$,
$V(\beta) = 2\theta_1(\beta)\theta_2(\beta)\psi_1'(\beta) + \psi_2'(\beta)\theta_2(\beta)$.

At $\beta = \beta_H$, we have $\theta_1(\beta_H) = 0$ and $\theta_2(\beta_H) = \sqrt{\psi_2(\beta_H)}$. Using these results, we can obtain

$P(\beta_H) = -2\psi_2(\beta_H)$, $Q(\beta_H) = 2\psi_1(\beta_H)\sqrt{\psi_2(\beta_H)}$,
$U(\beta_H) = \psi_3'(\beta_H) - \psi_1'(\beta_H)\psi_2(\beta_H)$ and $V(\beta_H) = \psi_2'(\beta_H)\sqrt{\psi_2(\beta_H)}$.

Now,

$$\begin{aligned}
\frac{d}{d\beta}(Re(\chi(\beta)))\mid_{\beta=\beta_H} &= \frac{Q(\beta_H)V(\beta_H) + P(\beta_H)U(\beta_H)}{P(\beta_H)^2 + Q(\beta_H)^2} \\
&= \frac{2\psi_1(\beta_H)\sqrt{\psi_2(\beta_H)} \times \psi_2'(\beta_H)\sqrt{\psi_2(\beta_H)} + (-2\psi_2(\beta_H))(\psi_3'(\beta_H) - \psi_1'(\beta_H)\psi_2(\beta_H))}{(-2\psi_{(}\beta_H))^2 + (2\psi_1(\beta_H)\sqrt{\psi_2(\beta_H)})^2} \\
&= \frac{\psi_1(\beta_H)\psi_2'(\beta_H) - \psi_3'(\beta_H) + \psi_1'(\beta_H)\psi_2(\beta_H)}{2(\psi_2(\beta_H) + (\psi_1(\beta_H))^2)} \\
&\neq 0, \quad if\ \psi_1(\beta_H)\psi_2'(\beta_H) - \psi_3'(\beta_H) + \psi_1'(\beta_H)\psi_2(\beta_H) \neq 0,
\end{aligned}$$

and $\chi_3(\beta_H) = -\psi_1(\beta_H) \neq 0$.

So, the transversality condition $\left(i.e.\frac{d}{d\beta}(Re(\chi_j(\beta))) \mid_{\beta=\beta_H} \neq 0, \quad j = 1, 2.\right)$ holds and the system (2.1) exhibits Hopf bifurcation at $\beta = \beta_H$. Hence, the theorem. □

4.4 Optimal control strategy

To analyze the impact of supplying additional food as a control strategy, we incorporate a time-dependent control variable $A(t)$, representing the quantity of additional food provided to the predator population. The control is bounded as $0 \leq A(t) \leq A_{max}$. The corresponding controlled system becomes:

$$\begin{aligned}
\frac{dS}{dt} &= aS - bS^2 - cSI - \frac{\beta SI}{\delta + S} - \frac{\alpha_1 SP}{1 + \gamma_1 S + \gamma_2 I + \lambda\eta A(t)}, \\
\frac{dI}{dt} &= \frac{\beta SI}{\delta + S} - \frac{\alpha_2 IP}{1 + \gamma_1 S + \gamma_2 I + \lambda\eta A(t)} - \mu I, \\
\frac{dP}{dt} &= \frac{(e_1\alpha_1 S + e_2\alpha_2 I + e_3\eta A(t))P}{1 + \gamma_1 S + \gamma_2 I + \lambda\eta A(t)} - mP.
\end{aligned} \tag{4.3}$$

The goal is to minimize the number of infected individuals $I(t)$ and the cost associated with implementing the control $A(t)$, over a finite time horizon $[0, T]$. This is achieved by minimizing the objective functional:

$$\mathbb{J}(A) = \int_0^T \left[a_1 I^2 + a_2 A^2 + a_3 P^2\right] dt, \tag{4.4}$$

where a_1, a_2, and a_3 are non-negative weight parameters balancing the importance of minimizing infection, control cost, and predator population, respectively. Interestingly, the term $a_1 I^2$ represents the disease burden, where the squared form penalizes high infection densities more severely and ensures differentiability of the objective function. The quadratic term $a_2 A^2$ penalizes the excessive use of additional food, thereby promoting economically efficient and ecologically sustainable strategies. Furthermore, the predator penalty term $a_3 P^2$ is included to prevent excessive growth of the predator population due to additional food supplementation, which could otherwise lead to ecological imbalance.

To solve this optimal control problem, we apply Pontryagin's Maximum Principle. First, we define the Hamiltonian function:

$$\begin{aligned}
\mathbb{H} = &\left[a_1 I^2 + a_2 A^2 + a_3 P^2\right] + \phi_1 \left[aS - bS^2 - cSI - \frac{\beta SI}{\delta + S} - \frac{\alpha_1 SP}{1 + \gamma_1 S + \gamma_2 I + \lambda\eta A}\right] \\
&+\phi_2 \left[\frac{\beta SI}{\delta + S} - \frac{\alpha_2 IP}{1 + \gamma_1 S + \gamma_2 I + \lambda\eta A} - \mu I\right] + \phi_3 \left[\frac{(e_1\alpha_1 S + e_2\alpha_2 I + e_3\eta A)P}{1 + \gamma_1 S + \gamma_2 I + \lambda\eta A} - mP\right],
\end{aligned} \tag{4.5}$$

where ϕ_1, ϕ_2 and ϕ_3 are the adjoint (or costate) variables corresponding to the state variables $S(t)$, $I(t)$, $P(t)$, respectively.

The dynamics of the adjoint variables are governed by:

$$\frac{d\phi_i}{dt} = -\frac{\partial \mathbb{H}}{\partial x_i}, \qquad i = 1,2,3, \tag{4.6}$$

i.e.,

$$\begin{aligned}
\frac{d\phi_1}{dt} &= -\frac{\partial \mathbb{H}}{\partial S} \\
&= -\Big[\phi_1\big\{a + 2bS - cI - \tfrac{\beta I}{\delta+S} + \tfrac{\beta SI}{(\delta+S)^2} - \tfrac{\alpha_1 P}{(1+\gamma_1 S+\gamma_2 I+\lambda\eta A)} + \tfrac{\alpha_1\gamma_1 SP}{(1+\gamma_1 S+\gamma_2 I+\lambda\eta A)^2}\big\} \\
&\quad +\phi_2\big\{\tfrac{\beta I}{\delta+S} - \tfrac{\beta SI}{(\delta+S)^2} - \tfrac{\alpha_2\gamma_1 IP}{(1+\gamma_1 S+\gamma_2 I+\lambda\eta A)^2}\big\} + \phi_3\big\{\tfrac{e_1\alpha_1 P}{(1+\gamma_1 S+\gamma_2 I+\lambda\eta A)} - \tfrac{e_1\alpha_1 SP}{(1+\gamma_1 S+\gamma_2 I+\lambda\eta A)^2}\big\}\Big]. \\
\frac{d\phi_2}{dt} &= -\frac{\partial \mathbb{H}}{\partial I} \\
&= -\Big[2a_1 I + \phi_1\big\{-cS - \tfrac{\beta S}{\delta+S} + \tfrac{\alpha_1\gamma_2 SP}{(1+\gamma_1 S+\gamma_2 I+\lambda\eta A)^2}\big\} + \phi_2\big\{\tfrac{\beta S}{\delta+S} - \tfrac{\alpha_2 P}{(1+\gamma_1 S+\gamma_2 I+\lambda\eta A)} \\
&\quad + \tfrac{\alpha_2\gamma_2 IP}{(1+\gamma_1 S+\gamma_2 I+\lambda\eta A)^2} - \mu\big\} + \phi_3\big\{\tfrac{e_2\alpha_2 P}{(1+\gamma_1 S+\gamma_2 I+\lambda\eta A)} - \tfrac{e_2\alpha_2 IP}{(1+\gamma_1 S+\gamma_2 I+\lambda\eta A)^2}\big\}\Big]. \\
\frac{d\phi_3}{dt} &= -\frac{\partial \mathbb{H}}{\partial P} \\
&= -\Big[2a_3 P - \phi_1\big\{\tfrac{\alpha_1 S}{(1+\gamma_1 S+\gamma_2 I+\lambda\eta A)}\big\} - \phi_2\big\{\tfrac{\alpha_2 I}{(1+\gamma_1 S+\gamma_2 I+\lambda\eta A)}\big\} + \phi_3\big\{\tfrac{(e_1\alpha_1 S+e_2\alpha_2 I+e_3\eta A)}{(1+\gamma_1 S+\gamma_2 I+\lambda\eta A)} - m\big\}\Big],
\end{aligned} \tag{4.7}$$

with transversality (terminal) conditions:

$$\begin{aligned}
\phi_1(T) &= 0 \\
\phi_2(T) &= 0 \\
\phi_3(T) &= 0.
\end{aligned} \tag{4.8}$$

The optimality condition is given by the following equation:

$$\frac{\partial \mathbb{H}}{\partial A} = 0, \tag{4.9}$$

leading to the nonlinear algebraic equation for the control A:

$$\begin{aligned}
&2a_2 A + \phi_1\Big\{\frac{\lambda\eta\alpha_1 SP}{(1+\gamma_1 S+\gamma_2 I+\lambda\eta A)^2}\Big\} + \phi_2\Big\{\frac{\lambda\eta\alpha_2 IP}{(1+\gamma_1 S+\gamma_2 I+\lambda\eta A)^2}\Big\} + \\
&\phi_3\Big\{\frac{e_3\eta P}{(1+\gamma_1 S+\gamma_2 I+\lambda\eta A)} - \frac{e_3\eta AP}{(1+\gamma_1 S+\gamma_2 I+\lambda\eta A)^2}\Big\} = 0,
\end{aligned} \tag{4.10}$$

i.e.,

$$\begin{aligned}
&2a_2\lambda^2\eta^2 A^3 + 4a_2\lambda\eta(1+\gamma_1 S+\gamma_2 I)A^2 + [2a_2(1+\gamma_1 S+\gamma_2 I)^2 + \phi_3 e_3\lambda\eta^2 \\
&-\phi_3 e_3\eta P]A + [\phi_1\lambda\eta\alpha_1 SP + \phi_2\lambda\eta\alpha_2 IP + \phi_3 e_3\eta P(1+\gamma_1 S+\gamma_2 I)] = 0.
\end{aligned} \tag{4.11}$$

It should be noted that equation (4.11) may theoretically have up to three positive roots. However, since the objective function aims to minimize the disease burden using the minimum amount of additional food supplement, we consider the smallest positive root of A as the relevant solution. Therefore, we define $A_c(t)$ as the least positive root of equation (4.11), from which the optimal control is constructed by projecting onto the admissible control set

$$A^*(t) = \min\Big\{\max\{0, A_c\}, A_{max}\Big\}. \tag{4.12}$$

This completes the formulation of the optimal control problem. The system comprising the state equations (4.3), the adjoint equations (4.7), the optimality condition (4.12), and the associated boundary and initial conditions forms a two-point boundary value problem, which can be solved numerically using iterative schemes such as the forward-backward sweep method. For a broader spectrum of readers, the outline of the numerical scheme for the forward-backward sweep method is provided below.

Forward-backward sweep method

In optimal control problems, the system dynamics are governed by the *state equations*, which form an initial value problem (IVP):

$$\frac{dx}{dt} = f(t, x(t), u(t)), \quad x(0) = x_0, \tag{4.13}$$

where $x(t)$ represents the state variables and $u(t)$ is the control variable.

The *co-state equations* (also called adjoint equations), derived from Pontryagin's Maximum Principle, typically form a boundary value problem (BVP):

$$\frac{d\phi}{dt} = -\frac{\partial H}{\partial x}, \quad \phi(T) = \phi_T, \tag{4.14}$$

where $\phi(t)$ are the co-state variables and H is the Hamiltonian function.

The challenge arises because the state equations are solved forward in time from $t = 0$ to $t = T$, while the co-state equations must be solved backward in time from $t = T$ to $t = 0$. Moreover, the optimal control depends on both state and co-state variables, resulting in a coupled system.

The **forward-backward sweep method** is an iterative numerical procedure to solve such coupled systems, described as follows:

(a) **Initialize control:** Start with an initial guess $u^{(0)}(t)$ over the interval $[0, T]$.

(b) **Forward sweep:** Using $u^{(k)}(t)$, solve the state equations forward in time:

$$\frac{dx^{(k)}}{dt} = f(t, x^{(k)}(t), u^{(k)}(t)), \quad x^{(k)}(0) = x_0.$$

(c) **Backward sweep:** With $x^{(k)}(t)$ and $u^{(k)}(t)$, solve the co-state equations backward in time:

$$\frac{d\phi^{(k)}}{dt} = -\frac{\partial H}{\partial x}\bigg|_{\left(x^{(k)}, u^{(k)}\right)}, \quad \phi^{(k)}(T) = \phi_T.$$

(d) **Control update:** Update the control using the optimality condition,

$$u^{(k+1)}(t) = \min_{\tilde{u} \in [0, u_{max}]} H(t, x^{(k)}(t), \phi^{(k)}(t), \tilde{u}).$$

(e) **Convergence check:** Repeat steps (b)-(d) until the control sequence $\{u^{(k)}\}$ converges within a desired tolerance.

This method leverages numerical integration schemes such as Runge-Kutta methods for both forward and backward sweeps and is effective for solving nonlinear optimal control problems where analytical solutions are generally not available.

5 Numerical results

In this section, we consider a hypothetical yet biologically feasible set of parameter values, as given below.
$a = 1, b = 1, c = 0.1, \beta = 0.6, \delta = 0.36, \alpha_1 = 0.005, \alpha_2 = 0.8, \gamma_1 = 0.1, \gamma_2 = 2.5, \lambda = 20, \eta = 0.1, A = 0, \mu = 0.4, e_1 = 0.2, e_2 = 0.15, e_3 = 0.22, m = 0.01.$

We use the parameter values specified above to investigate the qualitative behavior of system (2.1) through numerical simulations. Initially, we vary the infection rate β to observe how the system responds dynamically. For $\beta = 0.6$, the system exhibits a stable solution (see Figure 5.1). As we increase β to 0.7, the system transitions to a limit cycle, as shown in Figure 5.2. Further increasing the infection rate to $\beta = 0.95$ leads to a period-doubling behavior (see Figure 5.3). When β is raised to 1.7, the system displays chaotic dynamics, as illustrated in Figure 5.4. These results indicate that an increasing infection rate β can destabilize the system and drive it into chaotic regimes.

To better understand these transitions, we construct a bifurcation diagram with respect to β, treating it as the bifurcation parameter. The diagram, shown in Figure 5.5, covers the parameter range $\beta \in [0.5, 1.82]$ and reveals the complex dynamical structure of the system, including transitions from stability to chaos. Specifically, the system is disease-free for $\beta < 0.58$. Within the interval $\beta \in [0.58, 0.65)$, the system exhibits a stable focus, indicating convergence toward an endemic equilibrium. A limit cycle emerges for $\beta \in [0.65, 0.9)$, and for $\beta \in [0.9, 1.2)$, the system undergoes period-doubling oscillations. As β increases further to the range $[1.2, 1.82]$, the dynamics become increasingly complex, transitioning from double-period oscillations to higher-order periodic orbits and eventually to chaos.

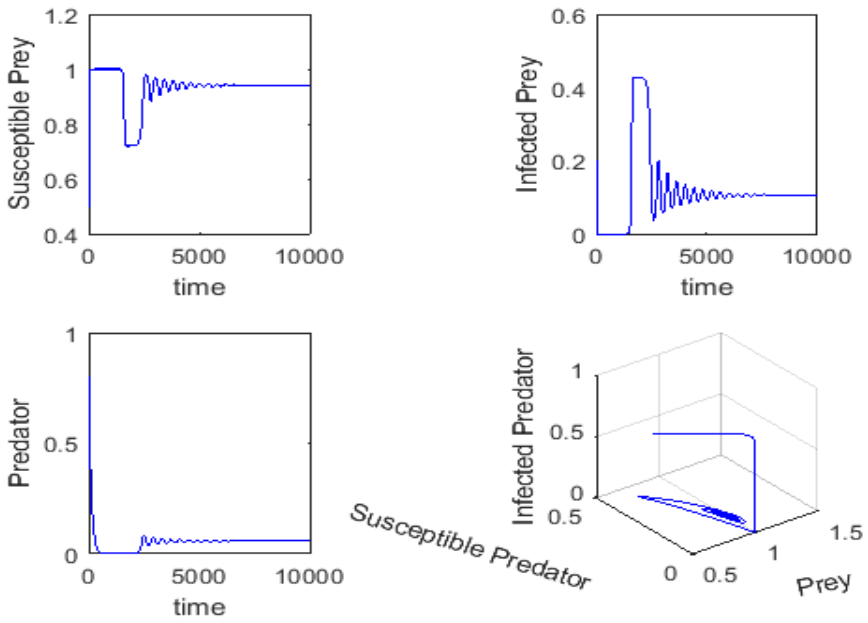

Figure 5.1: The system (2.1) is stable for $\beta = 0.6$ and $A = 0$ where $a = 1$; $b = 1$; $c = 0.01$; $\delta = 0.36$; $\alpha_1 = 0.005$; $\alpha_2 = 0.8$; $\gamma_1 = 0.1$; $\gamma_2 = 2.5$; $\mu = 0.4$; $\lambda = 20$; $\eta = 0.1$; $e_1 = 0.2$; $e_2 = 0.15$; $e_3 = 0.22$; $\mu = 0.4$; $m = 0.01$; with the initial condition $[S(0), I(0), P(0)] = [0.5, 0.2, 0.8]$.

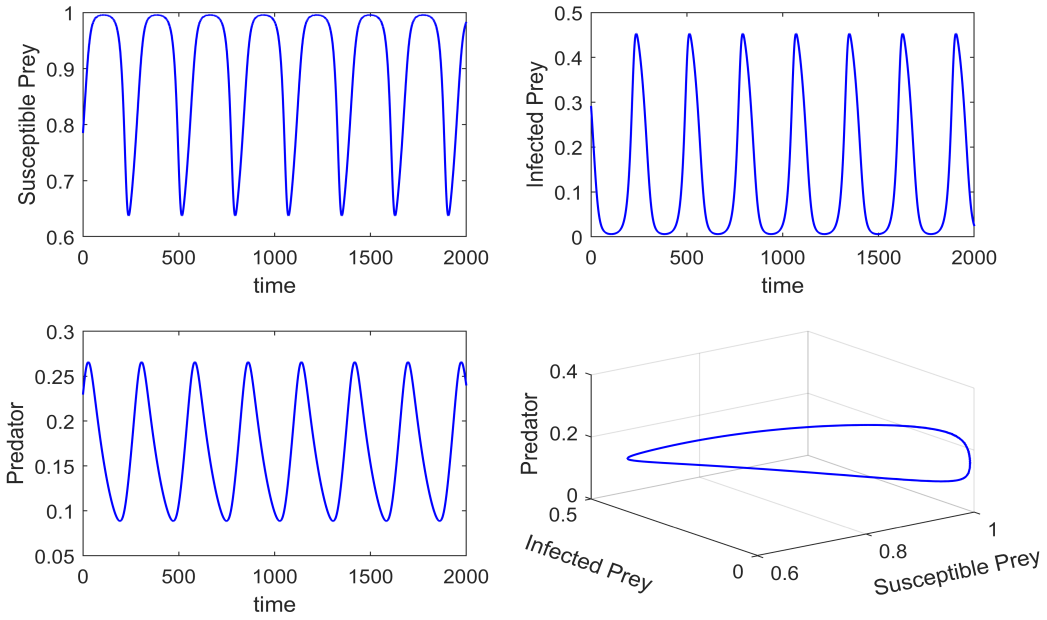

Figure 5.2: The figure shows limit cycle oscillation of the system (2.1) for $\beta = 0.7$ and other parameters values as in Figure 5.1

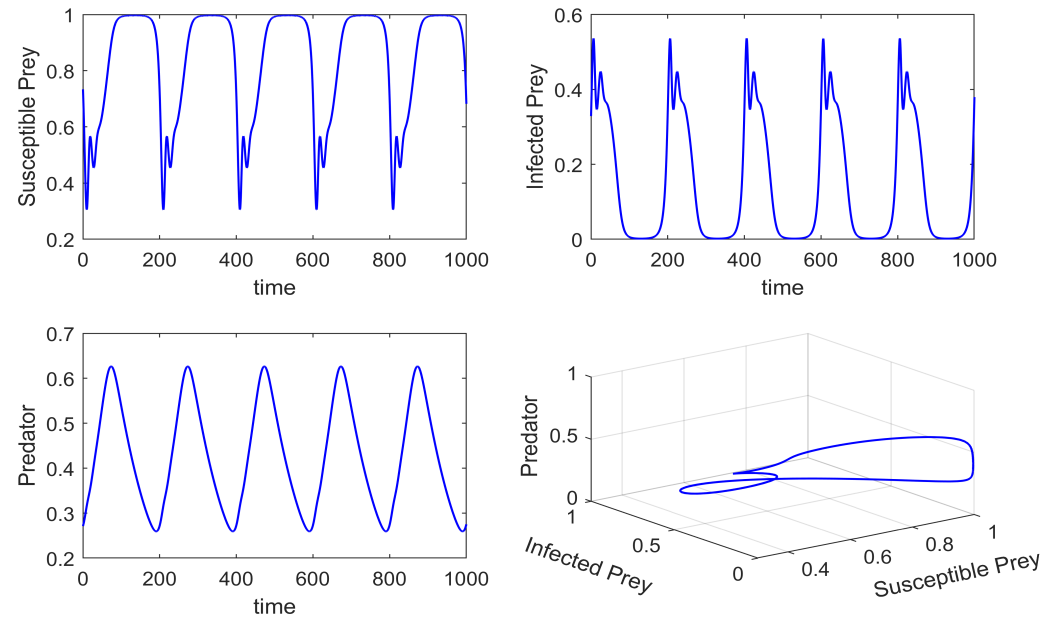

Figure 5.3: The system (2.1) shows period doubling oscillation for $\beta = 0.95$ and other parameters values as in Figure 5.1.

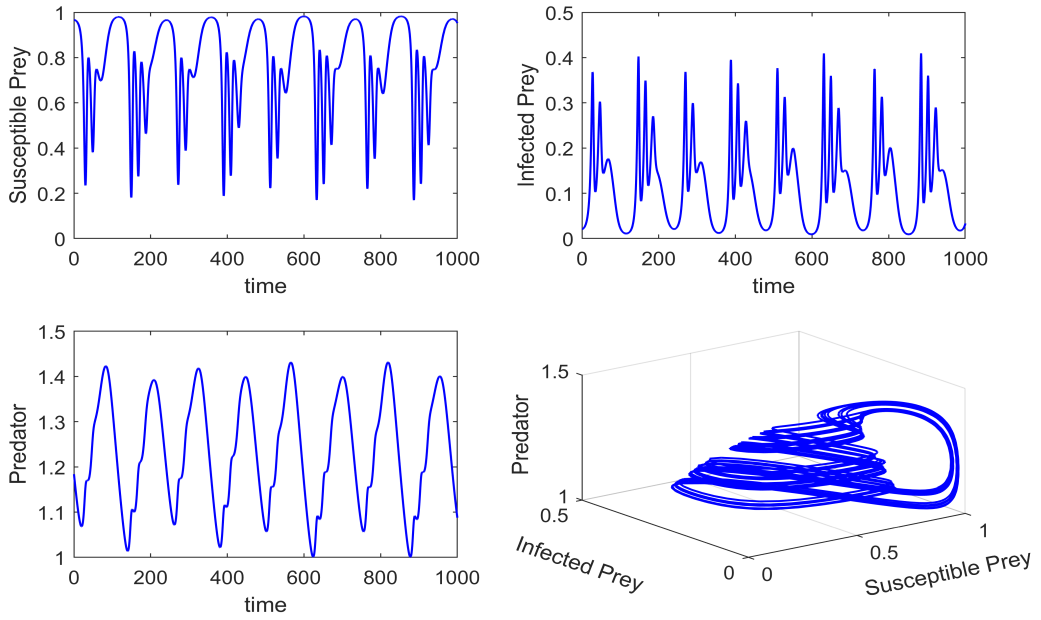

Figure 5.4: The system (2.1) shows chaos for $\beta = 1.7$ and other parameters values as in Figure 5.1.

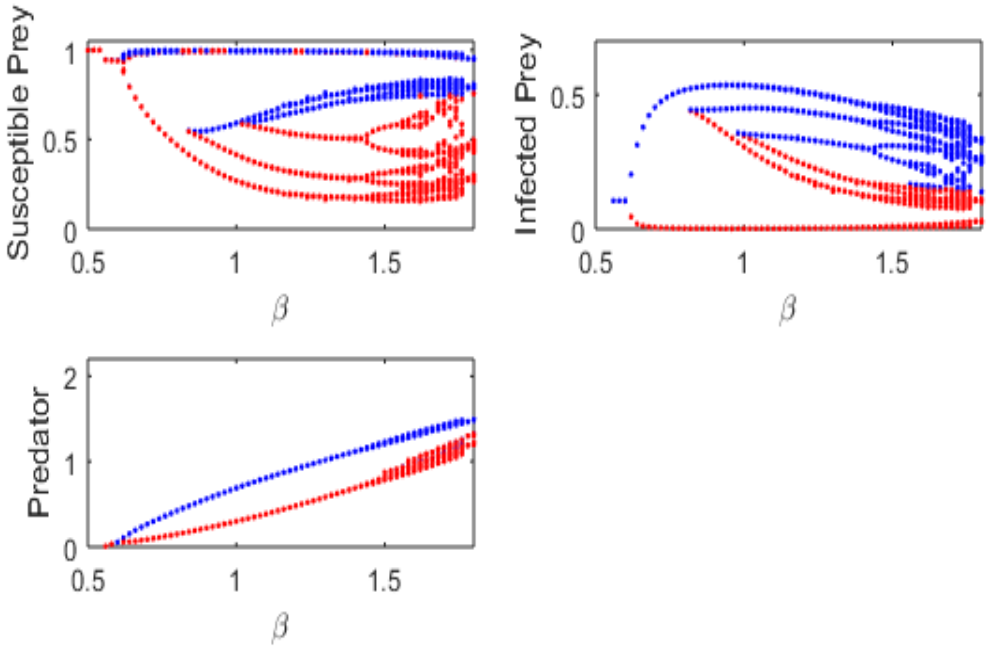

Figure 5.5: The bifurcation diagram for the system (2.1) with respect β, when the values of other parameter are remained same as in the Figure5.1.

Moreover, we compute the Poincaré map on the I-P plane by fixing $S = 0.5$, under the conditions $A = 0$ and $\beta = 1.7$ (see Figure 5.6). The scattered distribution of sampling points in the map confirms that the system exhibits chaotic behavior at $\beta = 1.7$ in the absence of additional food.

To further validate the presence of chaos, we calculate the system's maximum Lyapunov exponent at $\beta = 1.7$ (Figure 5.7). We begin by simulating the system dynamics and then compute the Lyapunov exponents from the resulting time series of the state variables. The numerical computation is performed using the method proposed by Wolf et al. [29,41], which allows for the estimation of non-negative Lyapunov exponents from experimental or simulated time series data. A positive value of the maximum Lyapunov exponent confirms the chaotic nature of system (2.1), as shown in Figure 5.7.

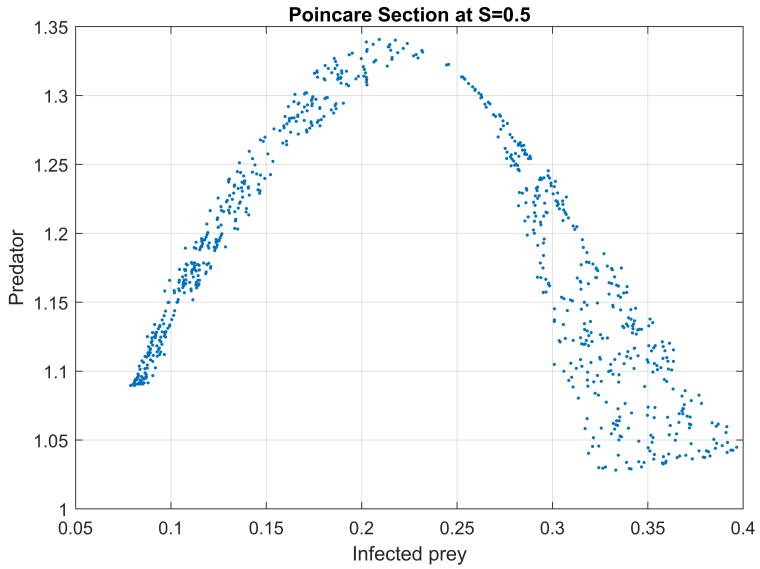

Figure 5.6: Figure shows the Poincare map of the system (2.1) in the I - P plane (S = 0.50).

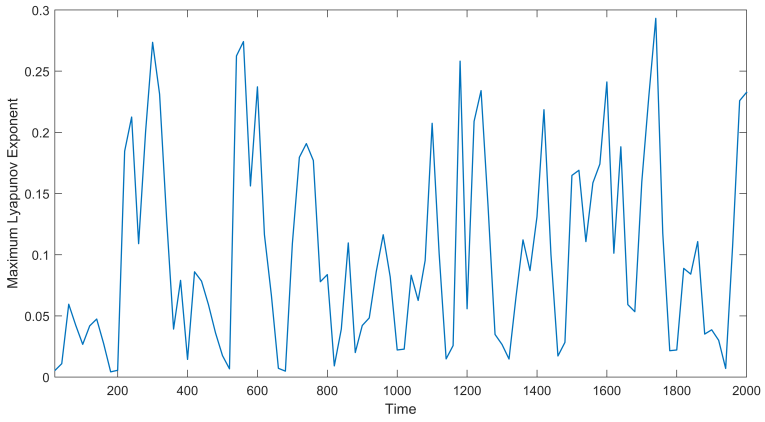

Figure 5.7: The maximum Lyapunov exponent of the system (2.1) for $\beta = 1.7$.

We now incorporate the additional food parameter A into system (2.1). When $A = 0.01$, the system exhibits chaotic behavior (see Figure 5.8). As we increase the value of A to 0.2, the system transitions to a two-periodic solution (Figure 5.9). Further increasing A to 0.6 leads to the emergence of a limit cycle, as shown in Figure 5.10. Finally, for $A = 0.8$, the system converges to a stable focus (Figure 5.11).

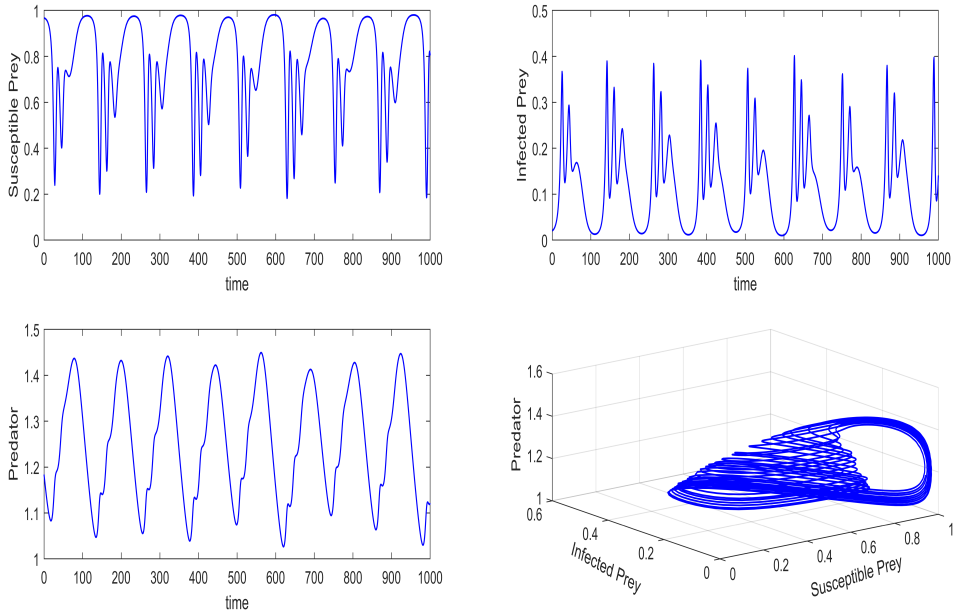

Figure 5.8: The system (2.1) shows chaos for the value of switching parameter $A = 0.01$ and other parameters values as in Figure 5.4.

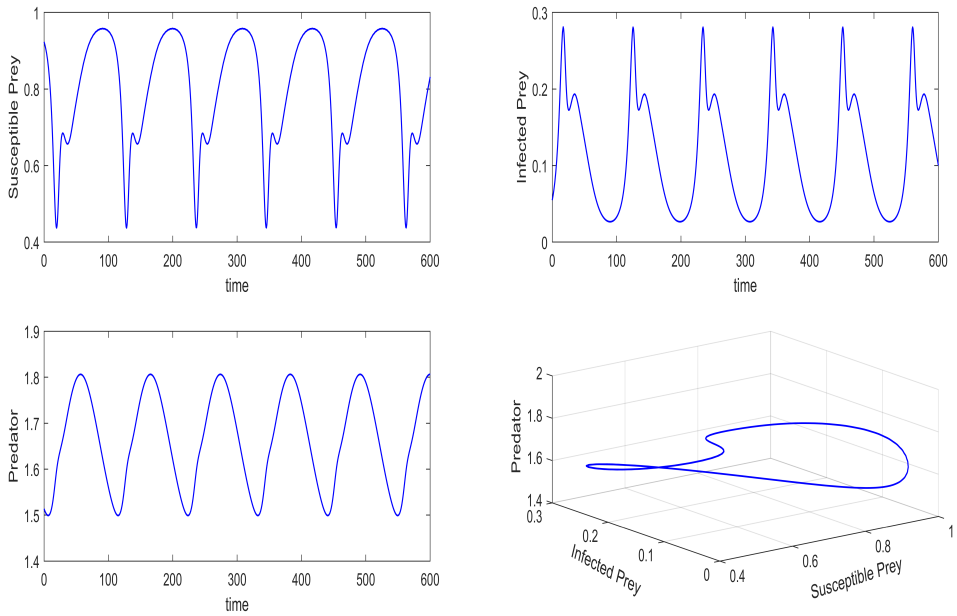

Figure 5.9: Existence of period-doubling oscillation around the interior equilibrium point E^* for the system (2.1) for $A = 0.2$, where the other values of parameter are remained same as in the Figure 5.4.

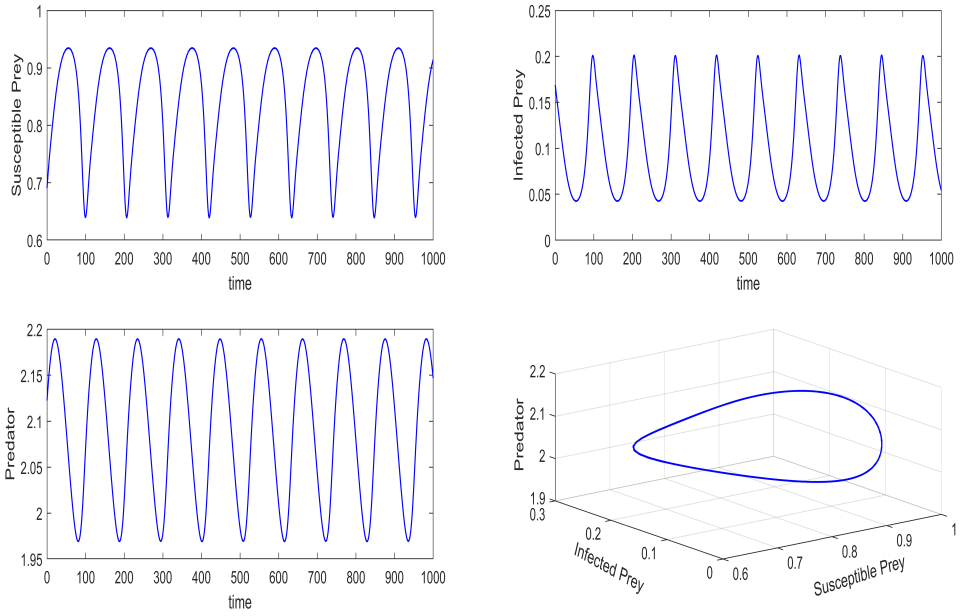

Figure 5.10: Existence of periodic oscillation around the interior equilibrium point E^* of the model (2.1) for $A = 0.6$, where the other values of parameter are fixed as in Figure 5.4.

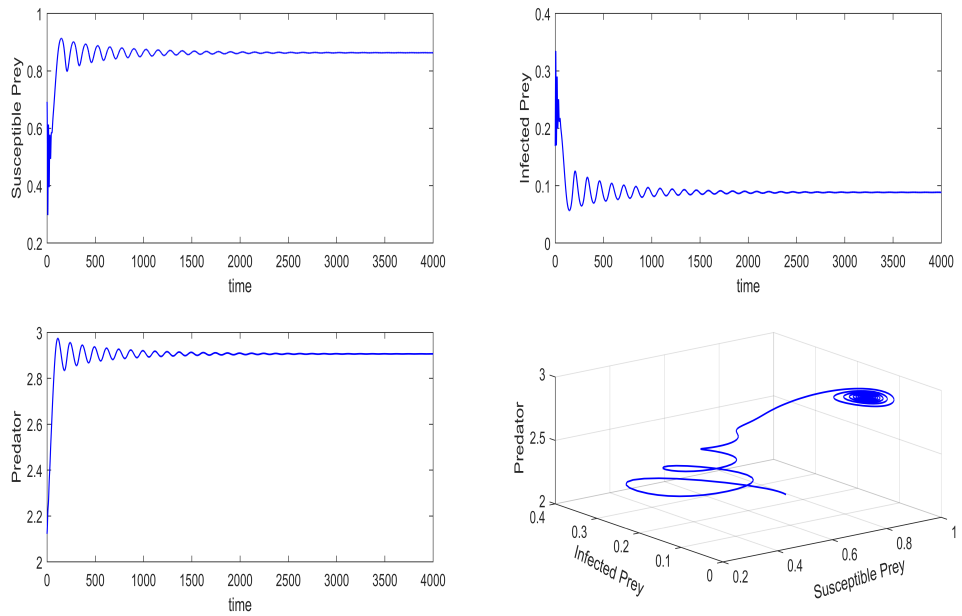

Figure 5.11: Stability of the interior equilibrium of the system (2.1), where $A = 0.8$ and the values of other parameter are same as in Figure 5.4.

To further illustrate the influence of additional food, we construct a bifurcation diagram of system (2.1) with respect to the parameter A over the interval $A \in [0, 1]$ (see Figure 5.12). The diagram reveals a rich variety of dynamical behaviors, transitioning from chaos to stable focus as A increases. Specifically, as A gradually increases, the system passes through a sequence of

dynamic regimes: from chaotic oscillations to period-doubling, then to limit cycle oscillations, and ultimately to a stable focus-indicating enhanced system stability.

Figure 5.12 shows that for $A \in [0, 0.09]$, the system exhibits high-period and chaotic oscillations; for $A \in (0.09, 0.21]$, it displays 2-periodic oscillations; and for $A \in (0.21, 0.72]$, it settles into limit cycle oscillations. Finally, for $A > 0.72$, the system stabilizes at an interior equilibrium point.

Furthermore, if the value of A is increased significantly-representing a higher external supply of additional food-we observe that for $A > 5$, the system reaches a disease-free stable equilibrium, meaning the infected prey population vanishes entirely (see Figure 5.13). This demonstrates that increasing the availability of additional food can lead to eradication of the disease within the prey population.

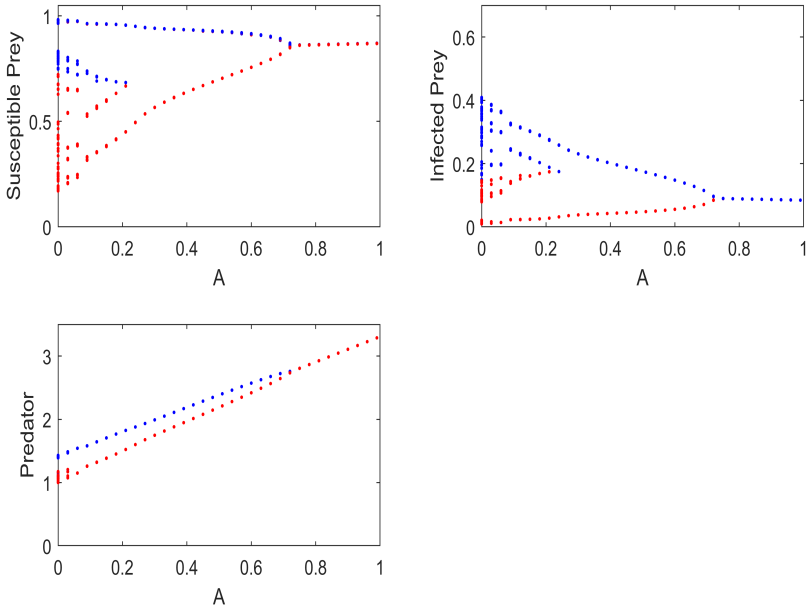

Figure 5.12: The bifurcation diagram for the system (2.1) with respect to A, when the values of other parameter are remained same as in the Figure 5.4.

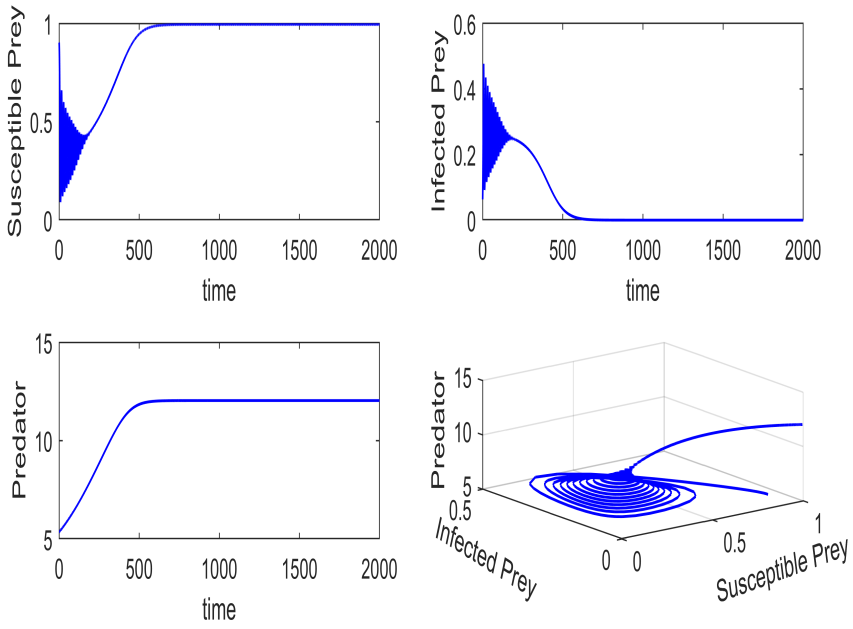

Figure 5.13: The system (2.1) shows disease-free stable focus for the value of additonal food parameter $A = 5.5$ and other parameters values as in Figure 5.4.

5.1 One-parameter bifurcation

5.1.1 One-parameter bifurcation with respect to infection rate (β)

At first we perform One-parameter bifurcation of the system (2.1) according to the disease infection rate β in the absence of additional food i.e. when $A = 0$. We have found transcritical bifurcation (BP) at $\beta = 0.552395$ where the predator population goes extinct. After slightly increasing the parameter value of β we have found supercritical Hopf ($H1_-$) bifurcation at $\beta = 0.612907$ since the first Lyapunov coefficient is negative ($l_1 = -0.167948$), which indicates occurrence of stable limit cycle. Between BP and Hopf bifurcation ($H1_-$) the system posses a unique positive interior equilibrium. Again, for further increasing the value of β, we have found supercritical Hopf bifurcation ($H2_-$) at $\beta = 2.506122$ which also shows stable limit cycle oscillation there. Further increasing of β the system shows subcritical Hopf bifurcation ($H3_+$) at $\beta = 3.426332$ since the first Lyapunov coefficient is positive ($l_1 = 4.220780$) and at this point the system shows unstable limit cycle oscillation. Additionally, for further increment of β, the system displays saddle node bifurcation (LP) at $\beta = 4.262811$. For further continuation of bifurcation diagram, the system shows another transcritical bifurcation (BP), when the predator population becomes extinction. The blue curve between $H2_-$ and $H3_+$ indicates stable coexistence equilibrium. All the above dynamical behavior are captured in Figure 5.14. Biological implications of the above bifurcations are described in Table 5.1.

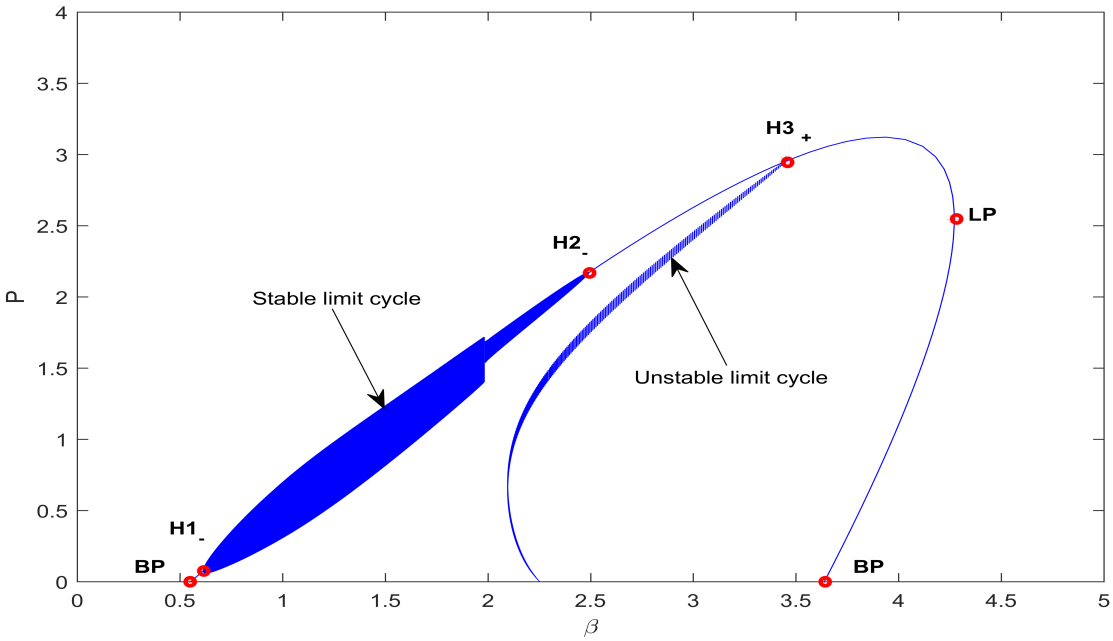

Figure 5.14: The bifurcation diagram of predator (P) with respect to disease infection rate (β) when additional food is zero i.e. $A = 0$; and values of all other parameters are same as in Figure 5.1. Here, BP; $H1_-$, $H2_-$ and $H3_+$ are transcritical bifurcation, supercritical and subcritical Hopf bifurcations, respectively and LP indicates the saddle-node bifurcation.

5.1.2 One-parameter bifurcation with respect to additional food (A)

Now we draw a bifurcation diagram with respect to additional food (A) and all other parameter values are same as that of Figure 5.1. It is observed that the system (2.1) shows supercritical Hopf bifurcation (H_-) at $(A = 0.717910)$, since the first Lyapunov coefficient is negative $(l_1 = -0.6252725)$. On the left side of the supercritical Hopf (H_-) point, the system exhibits stable limit cycle. For gradual increase in additional food, the system exhibits a transcritical bifurcation (BP) at $(A = 5)$. Therefore, the system experiences a transcritical bifurcation between interior equilibrium and disease-free equilibrium. Between H_- and BP, the system exhibits stable dynamics around the interior equilibrium point. We also observe that at right hand side of BP point (i.e. $A > 5$) system becomes entirely disease-free. For very small increment in A, the system shows a neutral saddle point labelled by H at $A = 5.000003$. All these dynamical features are captured in Figure 5.15.

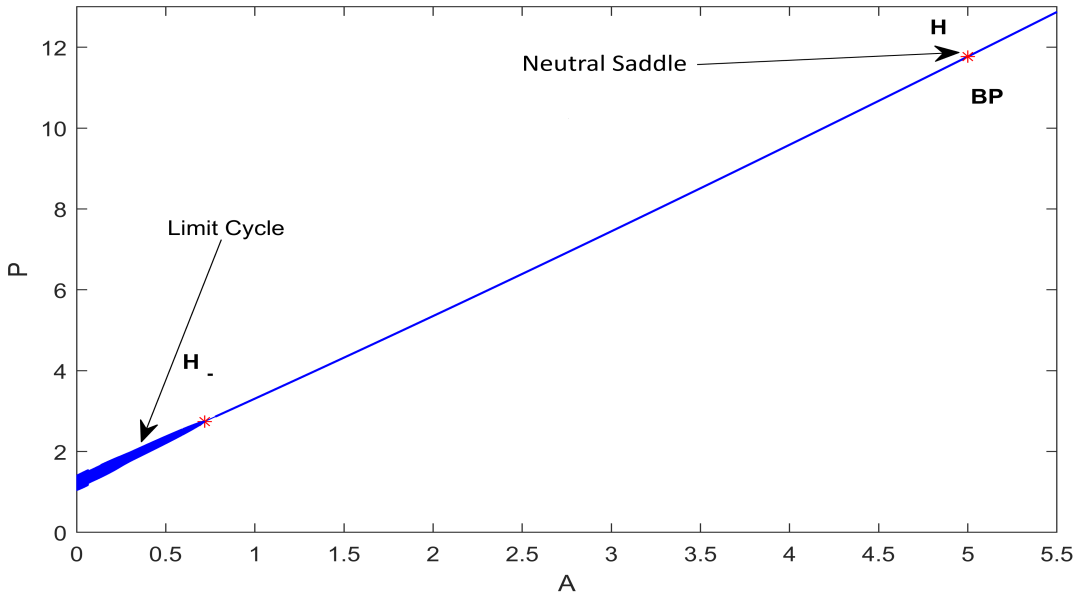

Figure 5.15: The bifurcation diagram of predator (P) w.r.t. additional food A, when $\beta = 0.58$; and values of all other parameters are same as in Figure 5.1.

5.1.3 One-parameter bifurcation with respect to predation rate on susceptible prey (α_1)

Considering the values $\beta = 1.7$ and $A = 1.2$ we now develop a bifurcation diagram relating to predation rate of predator to susceptible prey (α_1), keeping unchange all other parameter values being as in Figure 5.1. The system (2.1) exhibits supercritical Hopf bifurcation ($H1_-$) at $\alpha_1 = 0.029481$ as first Lyapunov coefficient is negative $(l_1 = -0.1251716)$. For further increment of α_1, again the system shows supercritical Hopf bifurcation ($H2_-$) with first Lyapunov coefficient $l_1 = -1.246089 \times 10^{-02}$ at $\alpha_1 = 0.04$. It is to be noted that on the left hand side of ($H1_-$) point, the system is stable around the coexisting steady state whereas the system displays stable limit cycle oscillations between these two supercritical Hopf bifurcations ($H1_-$ & $H2_-$). For a further increase of α_1, at $\alpha_1 = 0.044864$ a branch point (BP) or transcritical bifurcation occurs. It is interesting to note that between $H2_-$ and BP point system again becomes stable around the interior equilibrium. However, the system switches its stability from interior equilibrium to disease-free equilibrium point. That means at the right hand side of the transcritical bifurcation (BP) the system becomes disease-free ($I = 0$). The entire scenario has been demonstrated in the Figure 5.16.

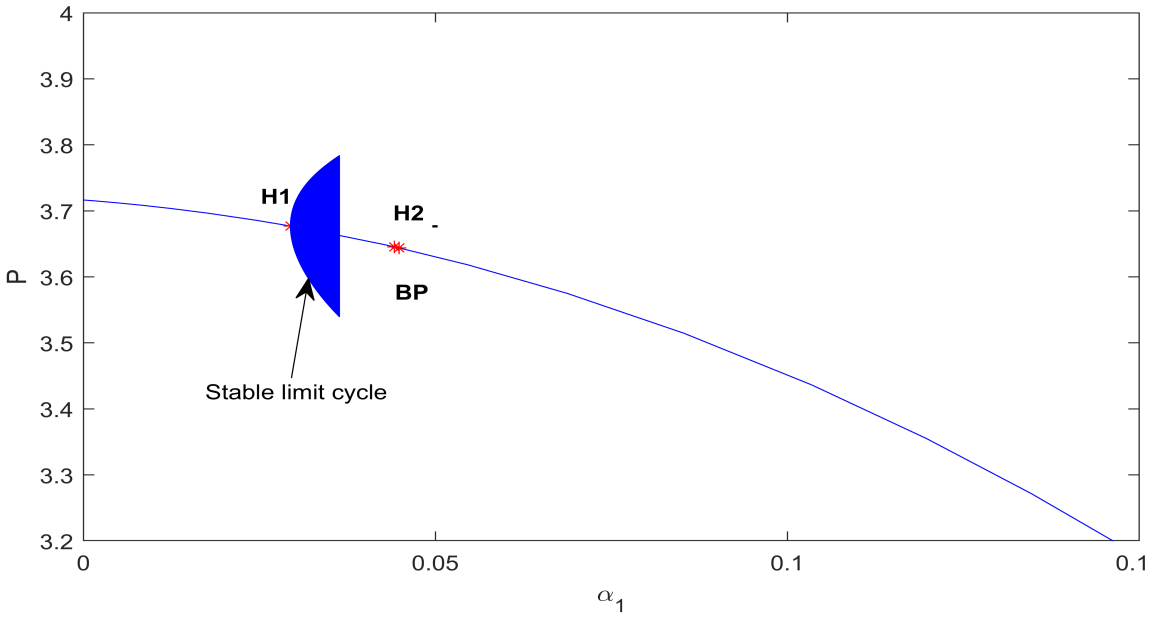

Figure 5.16: The One-parameter bifurcation diagram of predator (P) with respect to predation rate of predator to susceptible prey α_1 when $\beta = 1.7$ and $A = 1.2$; and values of all other parameters are same as in Figure 5.1.

5.1.4 One-parameter bifurcation with respect to predation rate on infected prey (α_2)

To investigate the impact of predation rate of predator to infected prey (α_2) on the population dynamics, we fix two parameter values of $\beta = 1.7$ and additional food $A = 1.2$, and other parameters remains same as in Figure 5.1. We draw the bifurcation diagram with respect to α_2, which displays that when the value of $\alpha_2 = 0.361775$ a saddle node bifurcation (LP) occurs, and two interior equilibrium points emerge in the system (2.1) (see Figure 5.17). For very small increment of α_2, system shows a subcritical Hopf bifurcation H_+ at $\alpha_2 = 0.364393$ and for further increase in α_2, system exhibits a transcrical bifurcation (BP) at $\alpha_2 = 0.378119$. Again if we increase in α_2, we find another Hopf bifurcation (H_-) at $\alpha_2 = 1.301133$, which is subcritical since first Lyapunove coefficient is negative. The system exhibits stable limit cycle oscillation on the right hand side of the bifurcation point H_-. Between these two Hopf bifurcation points, system is stable around an interior equilibrium point. From the Hopf point H_+, the system produces unstable limit cycle oscillations. On the left hand side of the saddle node bifurcation point interior equilibrium point doesn't exist since predator population extinct from the system.

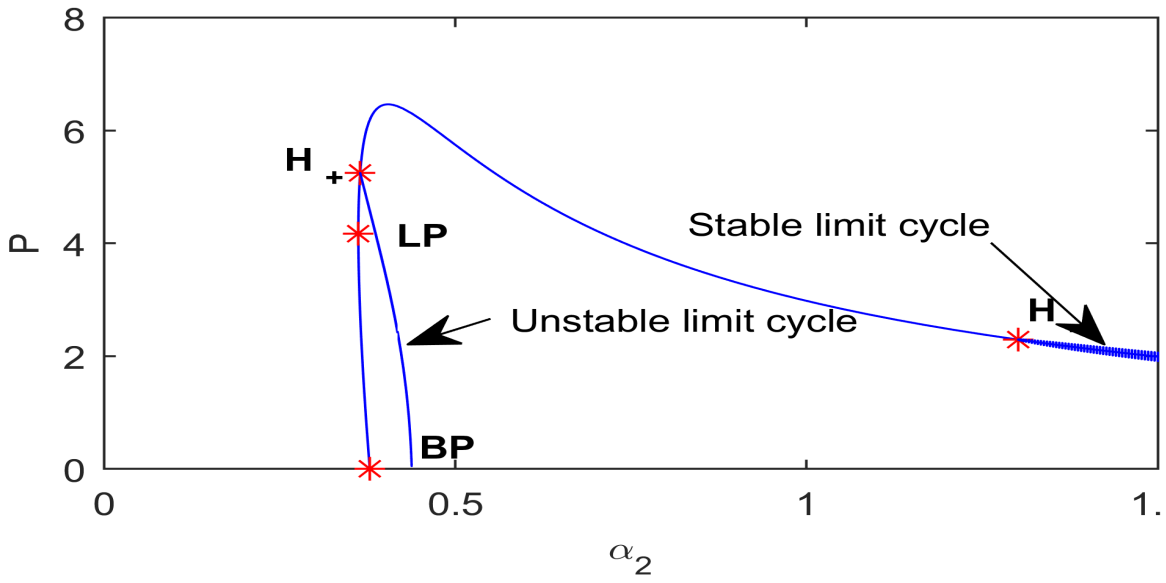

Figure 5.17: The bifurcation diagram of predator (P) with respect to predation rate of predator to infected prey α_2 when $\beta = 1.7$ and $A = 1.2$; and values of all other parameters are same as in Figure 5.1.

Table 5.1: Description of bifurcations and their biological implications.

Type of bifurcation	Biological implication
Hopf bifurcation (H)	An ecological system that was in a steady state starts to exhibit self-sustained oscillations (limit cycle oscillation) due to a small change in a parameter.
Supercritical Hopf bifurcation ($H1_-$)	For any initial population density, the system converges to a unique periodic solution, known as a stable limit cycle.
Supercritical Hopf bifurcation ($H1_+$)	For perturbations in the initial population density from the limit cycle oscillation (unstable limit cycle), the system converges either to a steady state or to another periodic solution.
Transcritical bifurcation (BP)	Two equilibrium points of the system, which always exist, exchange their stability (i.e., the stable one becomes unstable and the unstable one becomes stable) as the bifurcation parameter passes through a critical threshold value.
Sddle-node bifurcation (LP)	Either two steady states start to coexist, or they approach each other, collide, and vanish from the system. This means that beyond the critical value, the system may experience population extinction.

5.2 Two parameter bifurcation

5.2.1 Two-parameter bifurcation in the parametric plane $\beta - A$

Now we visualize the complex dynamic behaviour of the system (2.1) and perform a two parameter bifurcation in the parameter space $\beta - A$. Figure 5.18 represents the dynamical behaviour of the system as the infection rate β and additional food A vary along the $x-$ and $y-$axis, respectively. Different bifurcation curves divide $\beta - A$ parametric space into distinct dynamic regions. It is observed that when additional food A is low, and β is gradually increased, the system goes extinct except for the prey population i.e. only E_1 exists. The region R_1 colored in red is bounded by the transcritical bifurcation curve, and we have found a zero Hopf bifurcation point on that curve. Again, if we increase β, the system enters the R_5 region (green). Here, all populations coexist stably. For further increment of β, the system enters the R_2 region (pink), and this region is bounded by the Hopf bifurcation curve. Here all species coexist in an oscillating manner. For a further increase in β, the system gradually enters the R_3 (blue) and then R_4 (cyan) regions, respectively. These two regions are bounded by another Hopf bifurcation curve; here, the predator population goes to extinction while the other two prey population oscillate together. It is observed that incorporation of alternative food gradually stabilizes the system, and further increases in the alternative food parameter (i.e., above a critical value of $A = 5$) make the system disease-free and create a region which is colored in yellow marked as R_6.

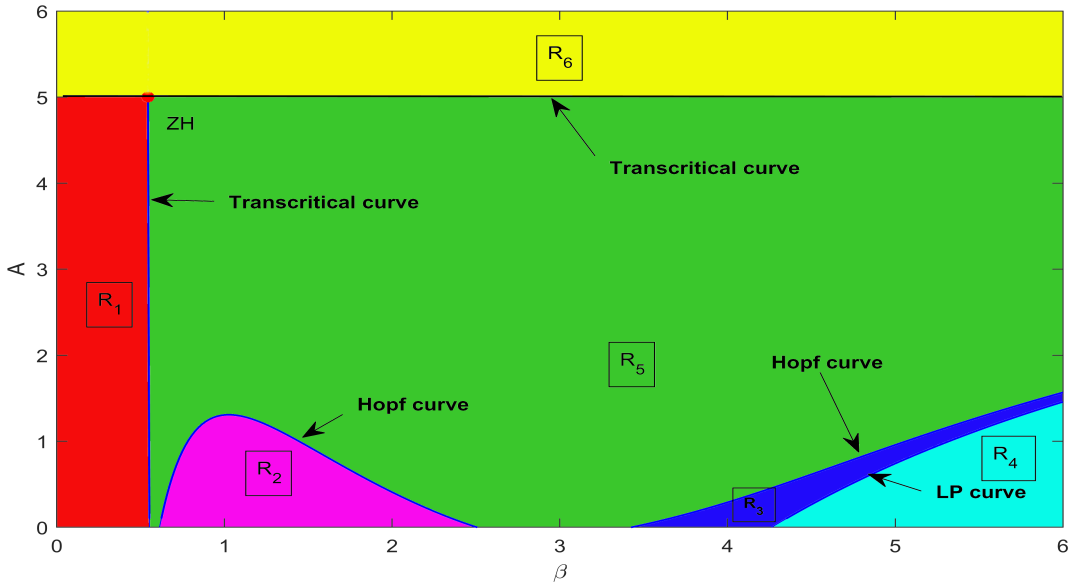

Figure 5.18: The two-parameter bifurcation diagram of the system with respect to disease infection rate of susceptible prey (β) and additional food (A) when the values of all other parameters are same as in Figure 5.1.

5.2.2 Two-parameter bifurcation in the parametric plane $\beta - \alpha_1$

Now we fix $A = 0.01$ and then draw a two-parameter bifurcation in the $\beta - \alpha_1$ parametric space. Various bifurcations are observed, namely saddle-node, Hopf, and transcritical bifur-

cations, as we vary the value of disease transmission rate β and predation rate α_1. The whole parametric space $\beta - \alpha_1$ is separated into several distinct dynamical domains by the bifurcation curves. In the Figure 5.19, we observed that when β is very small, the red region is occurred where the system is stable around the prey-only axial equilibrium. If β is increased slightly, the system enters the green region, where it is stable around the interior equilibrium point and all species coexist stably. With a further increase in β, the system transitions into the pink region. In this region all species of the system are oscillating together. The yellow region enclosed by Hopf bifurcation curves is disease-free zone. Here the system is stable around an infection-free equilibrium point. For sufficiently large value of β the system enters into blue and cyan region. The system exhibits limit cycle oscillation and here predator population extinct from the system.

It is observed that the system undergoes a zero-Hopf (ZH) bifurcation at which the LP curve and the Hopf curve meet tangentially. This zero-Hopf bifurcation occurs at $\beta = 5.487369$ and $\alpha_1 = 0.063908$. A zero-Hopf bifurcation is characterized by the presence of one zero eigenvalue and a pair of purely imaginary eigenvalues at the critical equilibrium point. In addition, several other codimension-two bifurcations are observed, including another ZH point at $\beta = 0.544000$ and $\alpha_1 = 0.054900$; a generalized Hopf (GH) bifurcation at $\beta = 6.880697$ and $\alpha_1 = 0.171451$; and a Bogdanov-Takens (BT) bifurcation at $\beta = 6.673923$ and $\alpha_1 = 0.091776$. The complete bifurcation scenario is illustrated in Figure 5.19.

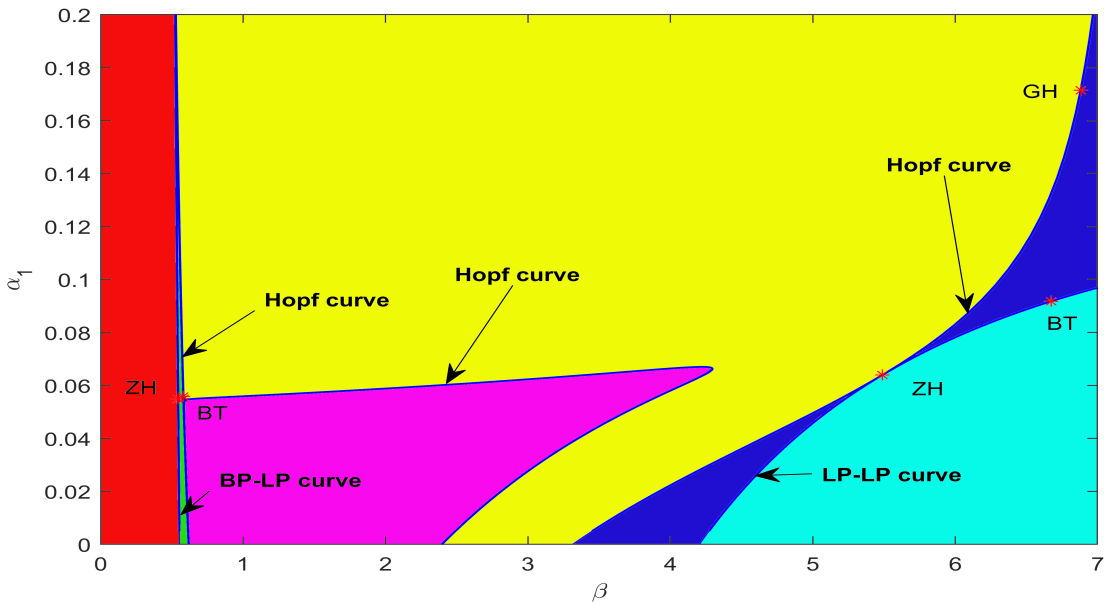

Figure 5.19: The two-parameter bifurcation diagram of the system with respect to disease infection rate (β) and predation rate to the susceptible prey (α_1), when the values of all other parameters are same as in Figure 5.1.

5.3 Optimal control of infection

To analyze the impact of additional food supply as a control strategy, we formulated the optimal control problem using the following parameter set: $a = 1$, $b = 1$, $c = 0.1$, $\beta = 0.6$, $\delta = 0.36$, $\alpha_1 = 0.005$, $\alpha_2 = 0.8$, $\gamma_1 = 0.1$, $\gamma_2 = 2.5$, $\lambda = 20$, $\eta = 0.1$, $\mu = 0.4$, $e_1 = 0.2$, $e_2 = 0.15$,

$e_3 = 0.22$, and $m = 0.01$. For these values, the uncontrolled system (2.1) exhibits a stable focus around the interior equilibrium.

The control variable $A(t)$, representing the time-dependent supply of additional food to the predators, is constrained by $0 \leq A(t) \leq 5.5$. The weight parameters in the objective functional are set as $a_1 = 1$, $a_2 = 1$, and $a_3 = 0.1$.

Figure 5.20 illustrates the time evolution of the susceptible prey $S(t)$, infected prey $I(t)$, and predator population $P(t)$ under the optimal control $A^*(t)$. The infection level $I(t)$ declines rapidly and approaches extinction over time, which represents a desirable outcome. Concurrently, the susceptible prey $S(t)$ increases and stabilizes, while the predator population $P(t)$ rises initially and subsequently stabilizes at a moderate level.

The optimal control profile $A^*(t)$ shows that a high supply of additional food is applied initially to support the predator population and aid in infection control. As the infection diminishes and predator dynamics stabilize, the control effort gradually decreases to zero.

The bottom row of Figure 5.20 presents the time trajectories of the adjoint variables $\phi_1(t)$, $\phi_2(t)$, and $\phi_3(t)$, which reflect the marginal cost associated with the respective state variables. The trajectories of ϕ_2 and ϕ_3 are notably negative at the start, indicating a high cost associated with the infected prey and predator populations early in the time frame. Over time, all costate variables converge to zero, consistent with the terminal conditions.

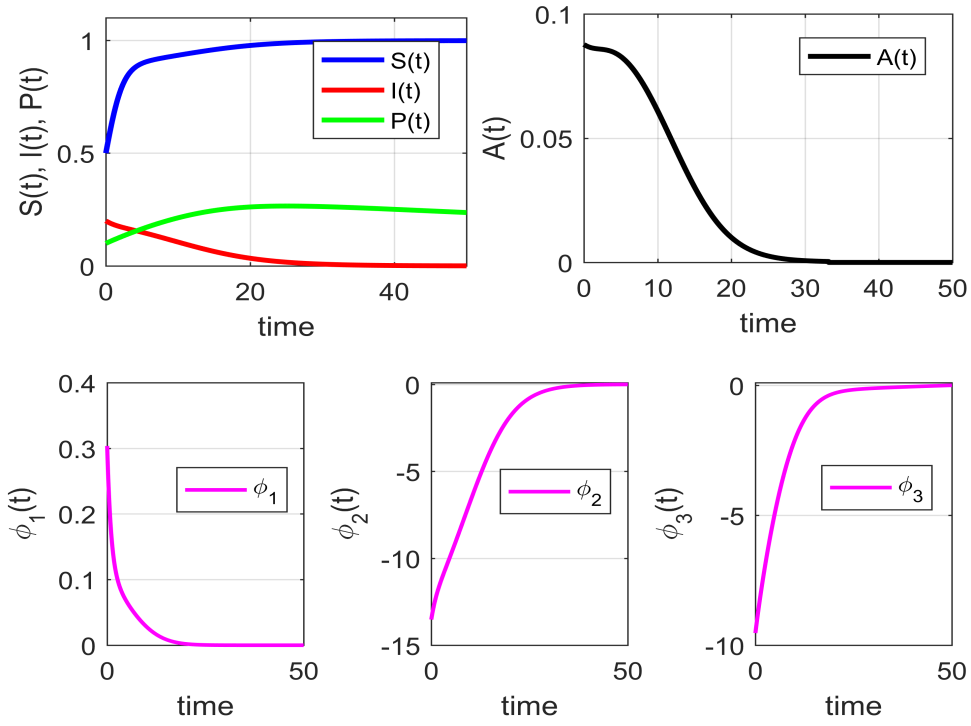

Figure 5.20: Time series of the state variables (top-left), optimal control $A(t)$ (top-right), and adjoint variables $\phi_1(t)$, $\phi_2(t)$, and $\phi_3(t)$ (bottom row) for the parameter set: $\beta = 0.6$, $A_{\max} = 0.2$. The optimal control reduces the infection $I(t)$ while supporting predator $P(t)$ and prey $S(t)$ populations efficiently.

To evaluate the influence of increased disease transmission, we conducted optimal control simulations for $\beta = 0.7$ under the constraint $0 \leq A(t) \leq 0.2$. Notably, in the absence of

control, the system exhibits persistent limit-cycle oscillations at $\beta = 0.7$ due to strong nonlinear interactions among the susceptible prey, infected prey, and predator populations. However, as shown in Figure 5.21, the implementation of the optimal food-based intervention effectively suppresses these oscillations.

The upper-left panel illustrates the time evolution of $S(t)$, $I(t)$, and $P(t)$, where the infection is significantly reduced and ultimately eradicated, while the susceptible and predator populations stabilize. The optimal control profile $A(t)$, depicted in the upper-right panel, rises smoothly to a peak below the upper bound and declines to zero as the infection diminishes. The adjoint variables $\phi_1(t)$, $\phi_2(t)$, and $\phi_3(t)$, shown in the lower panels, guide the control process and satisfy the transversality conditions at the final time.

These results demonstrate that optimal control not only mitigates disease spread but also converts the long-term oscillatory behavior into a stable equilibrium, thereby enhancing system resilience even under higher infection pressure. Furthermore, we simulated the optimal control model (4.3) with $\beta = 1.65$ and $A_{\max} = 5.5$ (see Figure 5.22), confirming that the optimal control scheme presented in Section 4.4 is robust.

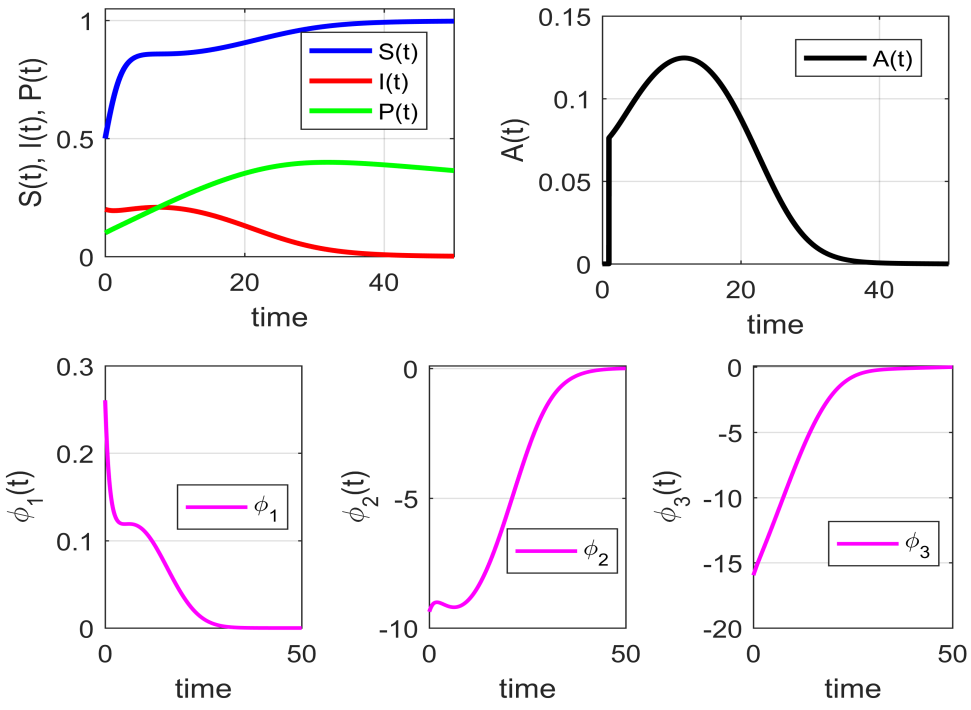

Figure 5.21: Time series of the state variables (top-left), optimal control $A(t)$ (top-right), and adjoint variables $\phi_1(t)$, $\phi_2(t)$, and $\phi_3(t)$ (bottom row) for the parameter set: $\beta = 0.7$, $A_{\max} = 0.2$. The optimal control reduces the infection $I(t)$ while supporting predator $P(t)$ and prey $S(t)$ populations efficiently.

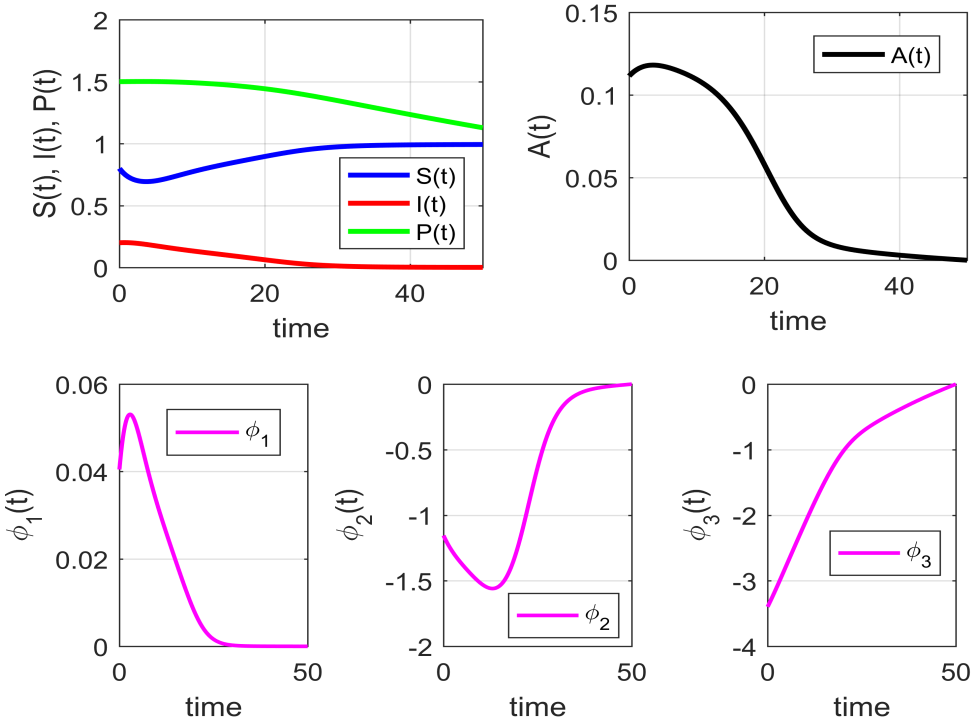

Figure 5.22: Time series of the state variables (top-left), optimal control $A(t)$ (top-right), and adjoint variables $\phi_1(t)$, $\phi_2(t)$, and $\phi_3(t)$ (bottom row) for the parameter set: $\beta = 1.65$, $A_{\max} = 5.5$. The optimal control reduces the infection $I(t)$ while supporting predator $P(t)$ and prey $S(t)$ populations efficiently.

These results highlight the effectiveness of optimal control in managing disease prevalence within a predator-prey ecosystem by judiciously adjusting the food supply to predators. This strategy achieves a balance between minimizing infection and maintaining stable predator-prey dynamics.

It is important to note that the food-based control considered here is ecologically feasible when the supplemental food supports predator survival without replacing their predation on both susceptible and infected prey. In practice, such strategies are already employed in integrated pest management and wildlife disease control. For instance, supplementary feeding can sustain populations of predatory fish that consume diseased or parasite-carrying fish, thereby controlling the spread of infection among smaller fish.

6 Conclusion

In this study, we analyzed an eco-epidemiological model comprising susceptible prey, infected prey, and predators, with a focus on the role of additional food provided to the predator population. The model incorporates nonlinear disease transmission and a generalized Holling type II functional response. Our results demonstrate that disease transmission can destabilize the system, potentially leading to chaotic dynamics. However, the inclusion of a constant external food source has a stabilizing effect and can suppress chaos.

Through bifurcation analysis, we observed transitions such as period-doubling, Hopf, and transcritical bifurcations as key parameters varied. The system exhibited rich dynamics, in-

cluding limit cycles and chaos, in the absence of additional food, particularly under high disease transmission rates. Conversely, increasing food availability induced period-halving bifurcations and ultimately stabilized the system. Beyond a critical threshold, additional food could eliminate the infected prey population entirely, resulting in a disease-free equilibrium.

To enhance the model's practical relevance, we introduced a time-dependent optimal control representing food supplementation. Using Pontryagin's Maximum Principle, we derived the necessary conditions for minimizing infection and intervention costs. Numerical simulations demonstrated that the optimal strategy effectively reduced disease prevalence and transformed oscillatory behavior into stable coexistence, even under conditions prone to chaos.

Overall, our findings highlight that strategic food supplementation can serve as a powerful ecological intervention for controlling disease and stabilizing predator-prey systems. This approach also opens new avenues for incorporating realistic resource-based controls in the management of eco-epidemiological dynamics.

Declarations

Availability of data and materials

Not applicable.

Funding

Not applicable.

Authors' contributions

S. Samanta: Conceptualized the study, Numerical simulations, Editing manuscript, Revision.
M.Y. Khan: Analytical calculation, Writing initial draft, Revision.
P. Sen: Analytical calculation, Writing initial draft, Revision.

Conflict of interest

The authors have no conflicts of interest to declare.

Acknowledgements

The authors are grateful to the anonymous referees for their valuable suggestions and comments, which significantly improved the quality of the paper.

References

[1] P.A. Abrams and J.D. Roth, *The effects of enrichment of three-species food chains with nonlinear functional responses*, Ecology, **75**(4) (1994), 1118–1130. DOI

[2] P. Akhtar, S. Karmakar and G. Samanta, *Exploring tri-trophic food chain model with toxicity and additional food: Unraveling bifurcation, chaos, density variation and bistability*, Int. J. Biomath., **2550024** (2025). DOI

[3] R.M. Anderson and R.M. May, *Population biology of infectious diseases: Part I*, Nature, **280**(5721) (1979), 361–367. DOI

[4] R.M. Anderson and R.M. May, *The invasion, persistence and spread of infectious diseases within animal and plant communities*, Philos. Trans. R. Soc. Lond. B Biol. Sci., **314**(1167) (1986), 533–570. DOI

[5] R. Arditi and L.R. Ginzburg, *Coupling in predator-prey dynamics: ratio-dependence*, J. Theor. Biol., **139**(3) (1989), 311–326. DOI

[6] H. Baek, *Species extinction and permanence of an impulsively controlled two prey one-predator system with seasonal effects*, Biosystems, **98**(1) (2009), 7–18. DOI

[7] J.K. Baum and B. Worm, *Cascading topdown effects of changing oceanic predator abundances*, Journal of Animal Ecology, **78**(4) (2009), 699–714. DOI

[8] S. Biswas, M. Saifuddin, S.K. Sasmal, S. Samanta, N. Pal, F. Ababneh and J. Chattopadhyay, *A delayed prey-predator system with prey subject to the strong Allee effect and disease*, Nonlinear Dynamics, **84** (2016), 1569–1594. DOI

[9] D.E., Burkepile and J.D. Parker, *Recent advances in plant-herbivore interactions*, F1000Research, **6** (2017), 119. DOI

[10] A. Casadevall and L. Pirofski, *Hostpathogen interactions: the attributes of virulence*, The Journal of infectious diseases, **184**(3) (2001), 337–344. DOI

[11] H.D. Crofton, *A model of host-parasite relationships*, Parasitology, **63**(3) (1971), 343–364. DOI

[12] P.H. Crowley and E.K. Martin, *Functional responses and interference within and between year classes of a dragonfly population*, J. North Am. Benthol. Soc., **8**(3) (1989), 211–221. DOI

[13] S. Gakkhar, B. Singh and R.K. Naji, *Dynamical behavior of two predators competing over a single prey*, Biosystems, **90**(3) (2007), 808–817. DOI

[14] D. Greenhalgh and M. Haque, *A predator-prey model with disease in the prey species only*, Math. Methods Appl. Sci., **30**(8) (2007), 911–929. DOI

[15] K. Hadeler and H.I. Freedman, *Predator-prey population with parasite infection*, J. Math. Biol., **27**(6) (1989), 609–631. DOI

[16] J.K. Hale and S.M.V. Lunel, *Introduction to functional differential equations*, Vol. 99, Springer Science & Business Media, 2013. URL

[17] H.W. Hethcote, W. Wang, L. Han and Z. Ma, *A predator-prey model with infected prey*, Theor. Popul. Biol., **66**(3) (2004), 259–268. DOI

[18] F.M. Hilker and K. Schmitz, *Disease-induced stabilization of predator-prey oscillations*, J. Theor. Biol., **255**(3) (2008), 299–306. DOI

[19] C.S. Holling, *The functional response of predators to prey density and its role in mimicry and population regulation*, Mem. Entomol. Soc. Can., **97**(S45) (1965), 5–60. DOI

[20] R.D. Holt and J.H. Lawton, *The ecological consequences of shared natural enemies*, Annu. Rev. Ecol. Syst., **25** (1994), 495–520. URL

[21] C. Ji and D. Jiang, *Analysis of a predator-prey model with disease in the prey*, Int. J. Biomath., **6**(03) (2013), 1350012. DOI

[22] Z. Kabata, *Parasites and Diseases of Fish Cultured in the Tropics*, Taylor and Francis, London, 1985. URL

[23] T.K. Kar and S.K. Chattopadhyay, *A focus on long-run sustainability of a harvested prey predator system in the presence of alternative prey*, Comptes Rendus Biologies, **333**(11-12) (2010), 841–849. DOI

[24] B.W. Kooi, G.A. van Voorn and K.P. Das, *Stabilization and complex dynamics in a predator-prey model with predator suffering from an infectious disease*, Ecol. Complex. **8**(1) (2011), 113–122. DOI

[25] A.J. Lotka, *Elements of Physical Biology*, Williams and Wilkins; Baltimore, New York, 1925. URL

[26] C. MacNeil, J.T. Dick, M.J. Hatcher, *et al.*, *Parasite-mediated predation between native and invasive amphipods*, Proc. R. Soc. Lond. Ser. B, Biol. Sci. **270**(1521) (2003), 1309–1314. DOI

[27] S. Mandal, A. Tripathi, R. Banerjee, F. Souna and P.K. Tiwari, *Ecological and epidemiological ramification of fear: Exploring deterministic and stochastic dynamics in a predator-prey system with predator switching and harvesting*, International Journal of Biomathematics, **2450109** (2024). DOI

[28] Ö. Östman, J. Eklöf, B.K. Eriksson, J. Olsson, P.O. Moksnes, U. Bergström, *Topdown control as important as nutrient enrichment for eutrophication effects in North Atlantic coastal ecosystems*, Journal of Applied Ecology, **53**(4), (2016) 1138–1147. DOI

[29] T. Park, *A matlab version of the Lyapunov exponent estimation algorithm of Wolf et al.*, Physica 16D, 1985. https://in.mathworks.com/matlabcentral/fileexchange/48084-wolf-lyapunov-exponent-estimation-from-a-time-series

[30] R.O. Peterson and R.E. Page, *Wolf density as a predictor of predation rate*, Swed. Wildl. Res. (Sweden), **1**, (1987) 771–773. URL

[31] P.C. van Rijn and M.W. Sabelis, *Impact of plant-provided food on herbivore-carnivore dynamics*, Plant-provided food for carnivorous insects: A protective mutualism and its applications, (2005) 223–266. DOI

[32] S. Roy, S. Alam and J. Chattopadhyay, *Role of nutrient bound of prey on the dynamics of predator-mediated competitive-coexistance*, Biosystems, **82**(2), (2005) 143–153. DOI

[33] S. Roy, S. Samanta, H. Nayak and P.K. Tiwari, *Deterministic vs. stochastic dynamics of a predator-prey system with disease in prey: Impact of fear and supplementary foods*, Int. J. Biomath. 2450047 (2024). DOI

[34] N. Sk, P.K. Tiwari, Y. Kang and S. Pal, *A nonautonomous model for the interactive effects of fear, refuge and additional food in a prey-predator system*, J. Biol. Syst., **29**(01) (2021), 107–145. DOI

[35] P.D. Spencer and J.S. Collie, *A simple predator-prey model of exploited marine fish populations incorporating alternative prey*, ICES J. Mar. Sci., **53**(3) (1996), 615–628. DOI

[36] P.D.N. Srinivasu, B.S.R.V. Prasad and M. Venkatesulu, *Biological control through provision of additional food to predators: A theoretical study*, Theor. Popul. Biol., **72**(1) (2007), 111–120. DOI

[37] P.D.N. Srinivasu and B.S.R.V. Prasad, *Time optimal control of an additional food provided predator-prey system with applications to pest management and biological conservation*, J. Math. Biol., **60**, 591–613 (2010). DOI

[38] S.Y. Strauss, *Indirect effects in community ecology: their definition, study and importance*, Trends Ecol. Evol., **6**(7) (1991), 206–210. DOI

[39] V. Volterra, *Variazioni e Fluttuazioni del Numero dIndivui in Specie Animali Conviventi*, Memorie della R. Accademia Lincei, **2** (1926), 31–113. URL

[40] E. Venturino, *Epidemics in predator-prey models: disease in the predators*, Math. Med. Biol., **19**(3) (2002), 185–205. DOI

[41] A. Wolf, J.B. Swift, H.L. Swinney and J.A. Vastano, *Determining Lyapunov exponents from a time series*. Physica D: Nonlinear Phenomena, **16**(3) (1985), 285–317. DOI

[42] Y. Zhang, J. Adams, *Topdown control of herbivores varies with ecosystem types*, Journal of Ecology, **99**(2) (2011), 370–372. DOI